

THE RESPONSE OF A GENERAL CIRCULATION CLIMATE MODEL TO
HIGH LATITUDE FRESHWATER FORCING IN THE ATLANTIC BASIN
WITH RESPECT TO
TROPICAL CYCLONE-LIKE VORTICES

by

VICTOR PAULIS

B.S. Florida Atlantic University, 1994
M.S. University of Central Florida, 1999

A dissertation submitted in partial fulfillment of the requirements
for the degree of Doctor of Philosophy in Modeling and Simulation
in the College of Sciences
at the University of Central Florida
Orlando, Florida

Summer Term
2007

Major Professor: Thomas Clarke

© 2007 Victor Paulis

ABSTRACT

The current cycle of climate change along with increases in hurricane activity, changing precipitation patterns, glacial melt, and other extremes of weather has led to interest and research into the global correlation or teleconnection between these events. Examination of historical climate records, proxies and observations is leading to formulation of hypotheses of climate dynamics with modeling and simulation being used to test these hypotheses as well as making projections. Ocean currents are believed to be an important factor in climate change with *thermohaline circulation* (THC) fluctuations being implicated in past cycles of abrupt change. Freshwater water discharge into high-latitude oceans attributed to changing precipitation patterns and glacial melt, particularly the North Atlantic, has also been associated with historical abrupt climate changes and is believed to have inhibited or shut down the THC overturning mechanism by diluting saline surface waters transported from the tropics. Here we analyze outputs of general circulation model (GCM) simulations parameterized by different levels of freshwater flux (no flux (control), 0.1 Sverdrup (Sv) and 1.0 Sv) with respect to tropical cyclone-like vortices (TCLVs) to determine any trend in simulated tropical storm frequency, duration, and location relative to flux level, as well as considering the applicability of using GCMs for tropical weather research. Increasing flux levels produced fewer storms and storm days, increased storm duration, a southerly and westerly shift (more pronounced for the 0.1 Sv level) in geographic distribution and increased activity near the African coast (more pronounced for the 1.0 Sv level). Storm intensities and tracks were not realistic compared to observational (real-life) values and is attributed to the GCM resolution not being fine enough to realistically simulate storm (microscale) dynamics.

ACKNOWLEDGEMENTS

I would like to thank Dr. Thomas Clarke, my advisor, for his support and understanding in providing the support to help bring this project to conclusion. I would also like to thank the other members of my committee, Drs. Peter Kincaid, Randall Shumaker, Mark Johnson and Erik Houglund for their help and support along the way. I would also like to thank Ronald Stouffer of GFDL and Jianjun Yin of COAPS for their help in providing the data for this project and Asuka Suzuki, of Georgia Tech, and Greg Holland of NCAR for their help in model storm detection, and also Mary Haley and Dennis Shea of NCAR, for their help with the NCAR Command Language (NCL). Finally, I need to thank my wife, Anna, for her assistance, understanding, and for putting up with me while working on this project.

TABLE OF CONTENTS

LIST OF FIGURES	ix
LIST OF TABLES	xi
LIST OF ACRONYMS/ABBREVIATIONS	xii
CHAPTER ONE: INTRODUCTION.....	1
Climate Change.....	1
Climate Cycles in the Past (Paleoclimatology).....	1
Current Climate, Global Warming and Human Contribution.....	4
Increased Tropical Cyclone Activity	4
Social and Economic Impacts.....	6
Climate Modeling	8
Research.....	9
Questions.....	9
Research Proposal.....	10
Rationale	11
CHAPTER TWO: LITERATURE REVIEW.....	12
Cycles of Climate Change	12
Ice Core Data	12
Vostok Ice Core	12
Climate Forcing	14
External Forcing Factors.....	15
Internal Forcing.....	17

Teleconnections	24
El Niño (La Niña) / Southern Oscillation (ENSO)	25
Thermohaline Circulation (THC) and Meridional Overturning Current (MOC)	26
Related Teleconnections	27
North Atlantic Oscillation (NAO)	27
Atlantic Multidecadal Oscillation (AMO)	28
Pacific Decadal Oscillation (PDO)	28
Madden-Julian Oscillation (MJO)	29
Tropical Cyclone Genesis	29
Anthropogenic Global Warming	30
Intergovernmental Panel on Climate Change (IPCC)	32
Links to Tropical Cyclone Activity	36
Modeling Climate and TC Activity	37
Climate Models	37
Energy Balance Models	38
Earth Models of Intermediate Complexity	38
General Circulation Models (GCMs)	39
Regional and Hybrid Models	40
Earth System Modeling Framework	41
Program for Climate Model Diagnoses and Intercomparison	41
Computational Resources for Climate Modeling	42
Temporal and Spatial Factors	42
Parallel Processing	43

Climate Data	44
Network Common Data Form (netCDF)	44
Analysis and Visualization	45
Tropical Storm Modeling.....	46
Tropical Cyclone-Like Vortices (TCLVs).....	47
Freshwater Forcing	51
CHAPTER THREE: METHODOLOGY	58
Research Focus	58
Procedures.....	58
Data.....	58
Preprocessing	59
TCLV Detection Script.....	60
CHAPTER FOUR: FINDINGS.....	65
Storm Statistics	65
Frequency.....	65
Storm Days.....	67
Duration	69
Location	72
Latitude & Longitude.....	72
Geographic Area	77
Track	80
Pressure, Wind, Vorticity & Temperature Anomaly	81
CHAPTER FIVE: CONCLUSION AND SUMMARY	83

Statistical Conclusions.....	83
Relevance of Results.....	85
Continuation and Suggestions	85
LIST OF REFERENCES	87

LIST OF FIGURES

Figure 1: Vostok time series with ice volume	13
Figure 2: Vostok time series with temperature and insolation	13
Figure 3: Vostok temperature (deuterium) power spectrum.....	16
Figure 4: Albedo: percentage of reflected sunlight for various surface conditions.....	20
Figure 5: Global Ocean Circulation.....	21
Figure 6: Three North Atlantic Glacial Ocean Circulation Modes.....	22
Figure 7: Time Series of THC Intensity (Sv) in Control Runs.....	53
Figure 8: Time Series of THC Intensity (Sv) in 0.1 Sv Water-Hosing Runs	54
Figure 9: Time Series of THC Intensity (Sv) in 0.1 Sv Water-Hosing Runs	55
Figure 10: Zonally averaged precipitation over the Atlantic Ocean.....	57
Figure 11: Average Monthly Storm Frequency	66
Figure 12: Average Annual Storm Frequency	66
Figure 13: Average Monthly Storm Days.....	68
Figure 14: Average Annual Storm Days.....	68
Figure 15: Average Monthly Storm Durations	70
Figure 16: Average Annual Storm Duration.....	70
Figure 17: Average Maximum Monthly Storm Durations	71
Figure 18: Average Annual Maximum Storm Durations	71
Figure 19: Latitude Distributions.....	73
Figure 20: Sorted Latitude Distributions	74
Figure 21: Longitude Distributions.....	75

Figure 22: Sorted Longitude Distributions	76
Figure 23: Average Area Frequency Distribution	78
Figure 24: Average Area Percentage Distribution.....	79
Figure 25: Average Area Percentage Distribution Summary	80

LIST OF TABLES

Table 1 2004, 2005, and Average Hurricane Statistics.....	5
Table 2 2004 and 2005 North Atlantic Hurricane Losses.....	7
Table 3 CCSM 3.0 Resolution and Run Times.....	44
Table 4 ECHM4.5 Basin Dependent & Independent TCLV Detection Thresholds.....	49
Table 5 TCLV Detection Threshold Values	63
Table 6 Average Storm Frequencies.....	67
Table 7 Average Annual Storm Days	67
Table 8 Average Annual Storm Duration	69
Table 9 Average Latitudes & Longitudes.....	72
Table 10 Average Zonal Storm Track Percentage.....	81
Table 11 Pressure, Wind, Vorticity, and Temperature Anomaly Values	82
Table 12 Summary of Average Statistics and Changes for 0.1 Sv & 1.0 Sv (vs. Control)	84

LIST OF ACRONYMS/ABBREVIATIONS

AR4	IPCC Fourth Assessment Report (2007)
BP	Before Present (typically before AD 2000)
D-O	Dansgaard-Oeschger (abrupt warming events)
EBM	Energy Balance Model
EMIC	Earth Model of Intermediate Complexity
ENSO	El Niño/Southern Oscillation
ESMF	Earth Systems Modeling Framework
GCM	General (or Global) Circulation Model
hPa	hectoPascal (\equiv 1 millibar (mb) - air pressure unit)
IPCC	Intergovernmental Panel on Climate Change
KYR (kyr)	kiloyear – thousand years
LGM	Last Glacial Maximum
LIA	Little Ice Age
Ma	Million years ago
MDR	Main development Region (for hurricanes)
MOC	Meridional Overturning Current (also THC)
NA	North Atlantic
NADW	North Atlantic Deep Water (THC/MOC)
NWP	Numerical Weather Prediction
PCMDI	Program for Climate Model Diagnoses & Intercomparison
SLP	Sea Level Pressure

SSS	Sea Surface Salinity
SST	Sea Surface Temperature
TAR	IPCC Third Assessment Report (2001)
TC	Tropical Cyclone (Hurricane in NA)
TCLV	Tropical Cyclone-Type Vortices
THC	Thermohaline Circulation (also MOC)
WRF	Weather Research & Forecast (model)

CHAPTER ONE: INTRODUCTION

Climate Change

Climate change is currently a predominant topic for discussion, inquiry and research. In the last decade, events such as strong storms, droughts, floods, as well as temperature extremes have fueled speculation about the nature and the cause of extreme weather and the overall trend in the earth's climate. Weather is thought of as the short-term (hours or days) state of the atmosphere-ocean-land with respect to wind, temperature, cloud cover, pressure, etc., while climate is the statistical composite or average of prevailing weather conditions, usually regional, and for a longer time period which can be months, seasons, decades, centuries or even longer. A historical perspective of climatic cycles is essential to understanding the nature of the recent changes in climate and weather extremes.

Climate Cycles in the Past (Paleoclimatology)

Historically, earth's climate can be measured in cycles of cooling and warming, or glaciation and melting. In glaciation, the earth cooled with glaciers pushing towards the equator, covering a greater area of the earth's surface. There have been four major glaciations, as well as many intervening and minor ones identified in the last [2,400 million years](#). The second oldest, and possibly the most severe, glaciation occurred between approximately 850 Ma (million years ago) to 635 Ma and may have iced over the entire globe, producing a *Snowball Earth*. The variability in earth's climate, especially over geologic time scales, is influenced by many factors, both external and internal. External factors include variations in solar radiation as well as earth's

orbital changes. Internal factors include plate tectonics, volcanic activity, and atmospheric composition.

By the *Pleistocene* epoch, approximately 1.8 million to 11,550 years BP (before present – typically AD 2000), the continental land masses were essentially in their present positions. The *Late Pleistocene* stage, from approximately 126,000 to 11,550 years BP, is of particular interest to climate researchers since it is the most recent climatic period characterized by repeated glacial cycles, including the *Last Glacial Maximum (LGM)* at approximately 20,000 to 18,000 years BP.

Abrupt climate changes during the last ice age (Late Pleistocene) have been identified from ice core data. Twenty three *Dansgaard-Oeschger (D-O) events* occurred between approximately 110,000 and 23,000 years BP. These were characterized in the Northern Hemisphere by rapid warming, usually over several decades, followed by gradual cooling over a longer period of time. Closely related are the *Heinrich events*, which occurred either 4 or 6 times during the last ice age, depending on data interpretation. Several Heinrich events occurred in the cold spells preceding the D-O rapid warming, and were characterized by a massive quantity of icebergs breaking off from the North American Laurentide ice sheet and traversing the North Atlantic towards Europe. It is speculated that the freshwater influx from the melting icebergs may have disrupted the North Atlantic THC, altering ocean currents and cooling the sub-tropical North Atlantic.

The end of the Pleistocene saw an abrupt and sudden return to glacial conditions known as the *Younger Dryas* stadial, also referred to as the *Big Freeze*, between approximately 12,700 to 11,500 years BP. A stadial is a period of colder temperature during an interglacial that is not sufficient in duration or strength to be considered a new glacial cycle. A prevailing theory on the cause of the Younger Dryas is that the North Atlantic *thermohaline circulation (THC)* was

significantly reduced or shutdown by a sudden influx of freshwater from Lake Agassiz, a huge freshwater lake in North America formed by glacial melts. The Younger Dryas transitions each occurred over approximately a decade, which can be considered fairly abrupt for climate change, especially compared to millennial climate cycles.

At approximately 11,550 years BP, late in the retreat of the Pleistocene glaciers, the current interglacial period and Holocene geological epoch began. Even though considered interglacial, the Holocene climate has shown considerable variability. The beginning of the Holocene evidenced a warming, with temperatures eventually becoming warmer than current conditions. Approximately 5,000 years BP, *Neoglaciation*, a period of cooler and wetter climate, not unlike today's, began. This is followed by a period of warming, called the *Medieval Climatic Optimum* at about 800-1300 AD. From about the 13th to the mid-19th centuries, came a period of cooling, known as *The Little Ice Age (LIA)*. By the end of the 19th century, the climate was warming again and the LIA was considered to have come to an end. The period since the end of LIA to present has seen a continued warming, with causes and consequences argued in the debate on *Global Warming*.

The dating and geographic distribution of paleoclimatic events is subject to a great deal of variability due to location of collection, resolution of dating methods, and interpretation of results. From the last millennium, events such as the Medieval Climatic Optimum and the LIA are biased by reliance on anecdotal and well documented evidence found in Europe. There is some question on how global or synchronous these events really are. The dates need to be considered as estimates with the realization that the timing and extent of these events will vary regionally.

The Holocene also dates the development of human civilization.

Current Climate, Global Warming and Human Contribution

Since the latter part of the 19th century, as mentioned above, earth's climate has been in a period of global warming where the average temperature has increased by over 1° F during the past century. It has also been observed that the rate of warming is increasing. Attribution of global warming has focused on natural variability and anthropogenic (human-induced) factors with the latest findings showing the anthropogenic contribution as very significant (discussed in Chapter 2).

Increased Tropical Cyclone Activity

The last decade has witnessed a significant increase in *Tropical Cyclone* (TC) activity. The North Atlantic (NA) basin has seen hurricanes (as TCs are called in the NA) increase in both frequency and intensity.

Compared with a period of low Atlantic hurricane activity (1971 to 1994), the period since 1995, except for a lull in 2006, has shown a marked increase. A study in 2001 (Goldenberg, Landsea, Mesta-Nunez & Gray, 2001) showed that since 1995 there was a doubling of overall activity with a 2.5-fold increase of major (Category 3 or greater) hurricanes and a 5-fold increase in hurricanes affecting the Caribbean. Since 2001, Atlantic hurricane activity, especially in 2004 and 2005 (shown in Table 1), has dramatically reinforced this trend that forecasters expect to continue for at least another decade or more

Table 1
2004, 2005, and Average Hurricane Statistics

Periods	<u>Hurricane Categories</u>			
	Named Storms (≥ 40 mph)	≥ Category 1 (≥ 74 mph)	≥ Category 3 (≥ 111 mph)	Category 5 (≥ 155 mph)
Average Year	10	6	2	0.3 – 0.5
2004	15	9	6	1
2005	28	15	7	4
<u>Increase</u>	<u>280%</u>	<u>250%</u>	<u>350%</u>	<u>~10× - 13×</u>

Information from the National Hurricane Center (NHC) [Archive of Hurricane Seasons](#)

The 2004 and 2005 NA hurricane seasons also broke numerous records including number of storms, location, and intensity.

- In 2004
 - The first TC (unofficially named Cyclone Catarina) since satellite observations began formed in the South Atlantic making landfall in Brazil
- In 2005
 - 28 named storms in the Atlantic. This was the first season, Atlantic or Pacific, to exhaust the list of names and to use the letters of the Greek alphabet
 - 15 storms that reached hurricane strength of Cat. 1 or greater
 - 7 major storms (hurricanes of Cat. 3 or greater) – 1 short of 1950 season’s record
 - 4 Cat.5 hurricanes

- 3 of the 6 most intense Atlantic storms on record formed during this season
- Hurricane Wilma underwent the most rapid intensification for a 24-hour period ever measured (from 980 mb to 882 mb – a fall of 98 mb) and is currently the most intense Atlantic storm on record (numerous Pacific typhoons have been more intense) with 882 mb minimum central pressure
- Hurricane Vince developed in the east Atlantic near Madeira, well away (north and east) from where hurricanes usually develop and was the first hurricane on record to make landfall in Spain

Social and Economic Impacts

A major, and arguably most important, impact of rapid climate change and increased TC activity is the socioeconomic cost incurred. Projections of extreme weather (Intergovernmental Panel on Climate Change, 2007a) and impacts on natural and biological systems (Intergovernmental Panel on Climate Change, 2007b) brought about by climate change threatens social and economic disruption. Projections of socioeconomic cost as a result of continuing climate change and suggestions for mitigation are found in the IPCC AR4 WGIII report (Intergovernmental Panel on Climate Change, 2007c).

The casualties and economic impact of the increased North Atlantic TC (hurricane) activity for 2004 and 2005 (the two most active years in the last decade) illustrates the costs of extreme weather. As shown in Table 2, the 2004 Atlantic hurricane season statistics estimate over 3100 casualties and economic losses of 42 billion dollars. The 2005 season estimates of

direct losses due to hurricane activity vary from 2000 to over 3600 casualties and over 110 billion dollars (record). Estimated losses directly attributed to hurricane Katrina alone are over 1600 casualties and 75+ billion dollars.

Table 2
2004 and 2005 North Atlantic Hurricane Losses

Year	<u>Estimated Direct Losses</u>	
	Casualties	Property Damage (\$US)
2004	> 3100	> \$42 billion
2005	2000 to > 3600	> \$110 billion (record)
<u>Katrina (2005)</u>	<u>> 1600</u>	<u>> \$75 billion</u>

Information from NOAA Technical Memorandum NWS [TPC-5](#)

Additionally, and not reflected in the tally above, are the indirect losses due to human suffering, population displacement, higher fuel costs and the political costs of ineptness in planning, preparation and response.

It should also be noted that during this period (1995 to present) of increased hurricane activity, the hurricane forecasts were exceeded in many, if not most of these years. This was especially evident in 2005, when the initial forecast by Gray (Dec. 3, 2004) predicted a slightly above average season (11 tropical storms and 6 hurricanes), but significantly less active than the 2004 season. Later (April 1, 2005) Gray raised his prediction slightly (13 tropical storms and 7 hurricanes) due to the absence of expected El Nino development. This was still way short of the actual season with 28 tropical storms and 15 hurricanes. This only suggests that we do not yet have a complete understanding of climatic processes to build models that would provide us with accurate forecasts.

Climate Modeling

Models, in general, are representations. Climate and weather models, through the use of quantitative methods, simulate the interactions of the atmosphere, land surface, oceans, and ice (very complex climate models may also simulate chemical interactions and biomes). They are used to study and validate our understanding of climate dynamics and for projections of future weather and climate. Weather models typically process real-time data for short term forecasts (several hours up to approximately ten days), while climate models are usually initialized with idealized data for specific scenarios of long term forecasts (months up to hundreds of years). The numerical basis of both weather and climate models is essentially the same. Some models, such as the Weather Research & Forecast ([WRF](#)) Model, are used for both real-time weather forecasts as well as longer-term climate research.

Climate models range in complexity from simple, one-dimensional energy-balance representations to fully-coupled *global circulation models (GCMs)*, also called *general circulation models*. While GCMs are the preferred tools for complex projections, simpler models are often used to validate GCMs as their complexity makes them more susceptible to bias. The Program for Climate Model Diagnosis and Intercomparison (PCMDI) at the Lawrence Livermore National Laboratory (LLNL) develops tools and methods to systematically account for significant disagreements between the increasingly more complex GCMs used in global climate change simulation and research.

Research

Questions

With respect to increased TC activity and its socioeconomic impact, the questions research is addressing include:

- What are the reasons for increased TC activity and how long will it last?
- How is global climate, including any changes, related to TC activity?
- What, if any, is the human contribution to climate change and to TC activity?
- What will the future climate (and TC activity) be in the short and long-term?
- What can we do to mitigate the negative effects climatic events such as TCs?

With respect to prediction and modeling of future climate changes and their effect on TCs, the following can be asked:

- What models and model requirements are appropriate to simulate climate change, both short term and long term?
- What models and model requirements are appropriate to simulate the microscale dynamics of tropical weather, especially TCs?
- What models, if any, are adequate to simulate both climate change and tropical weather?
- What are the model limitations and biases that need to be improved and corrected to achieve more accurate forecasts?

To address these questions requires:

- A better understanding of the physical processes in climate dynamics
- Building better models to verify and develop climate hypotheses for greater knowledge and understanding
- Use the gained knowledge and better models to more accurately predict future climatic events so that we can effectively plan, prepare for, and mitigate their negative effects

Research Proposal

Statistical correlations (teleconnections) between widely-separated climatic events (ENSO, etc.) and TC activity are being developed as tools in climate modeling and forecasting. Research has been conducted using various climate models, including fully-coupled GCMs to simulate the climate's TC response to anthropogenic CO₂ warming (Knutson & Tuleya, 1999) (Knutson & Tuleya, 2004) (Walsh & Katzfey, 1999). Research has also been done using GCMs on the Thermohaline Circulation (THC) and its response to global warming (Bryden, Longworth & Cunningham, 2005) and freshwater input (Ottera, Drange, Bentsen, Kvamsto & Jiang, 2004).

This focus of this research will be on the response of a GCM, with respect to TC activity, resulting from a simulation of freshwater flux forcing (water-hosing) in the high-latitude Atlantic basin, a situation that could be a consequence of global warming with glacial melt and changing precipitation patterns.

Rationale

Mitigation of social and economic losses due to extremes of climate such as hurricanes requires knowledge of their causes and reliable forecasts. Climate Models are the main tools we utilize to simulate future events and to provide feedback on our understanding of climate dynamics. It is hoped that this research would provide additional insight into climate dynamics and feedback concerning the validity of model mechanics with respect to the connection between tropical storms and high-latitude freshwater forcing.

CHAPTER TWO: LITERATURE REVIEW

Cycles of Climate Change

Ice Core Data

Data obtained from ice core compositions, primarily from Antarctica and Greenland, have provided climatologists with methods to date and quantify past climatic cycles (McGuffie & Henderson-Sellers, 2005). Stable and radioactive isotopes of hydrogen, carbon, oxygen, radon, as well as entrapped levels of dust, sodium, and methane are used to determine climatic changes. Concentrations of stable hydrogen and oxygen isotopes are proxies for local temperatures and ice volume, with concentrations of hydrogen-2 (^2H or deuterium D) proportional to temperature and concentrations of oxygen-18 (^{18}O) proportional to ice volume. Levels of entrapped dust, sodium, and methane provide information about the environment conditions at the time a particular core level formed. Decay rates of the radioactive isotopes, radon (^{222}Rn), carbon-14 (^{14}C), and tritium (^3H), are used to determine dates.

Vostok Ice Core

Until 2003, the longest ice core was drilled at the Vostok Station, a Russian research station in Antarctica, in the middle of the East Antarctic Ice Sheet. Analysis of the ice record (Petit et al., 1999) shows four glacial-interglacial cycles with a strong periodicity of $\sim 100,000$ years during the past 420,000 years. Time series plots of ice volume and temperatures are shown in Figures 1 and 2 below.

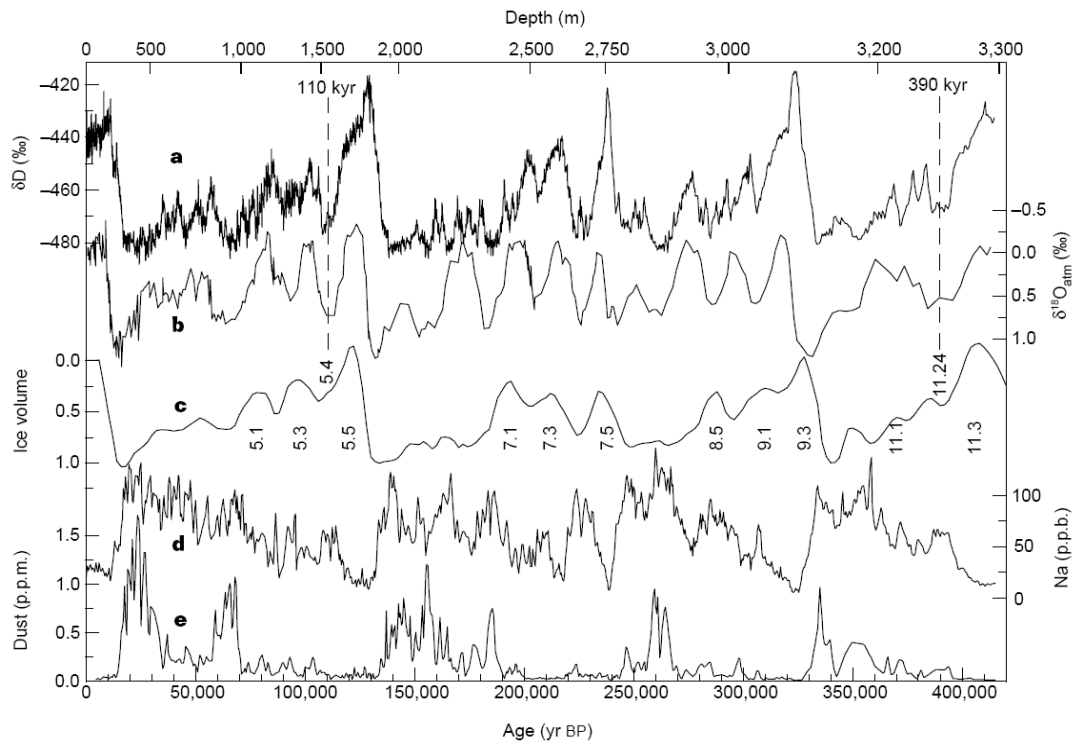


Figure 1: Vostok time series with ice volume
From (Petit et al. 1999)

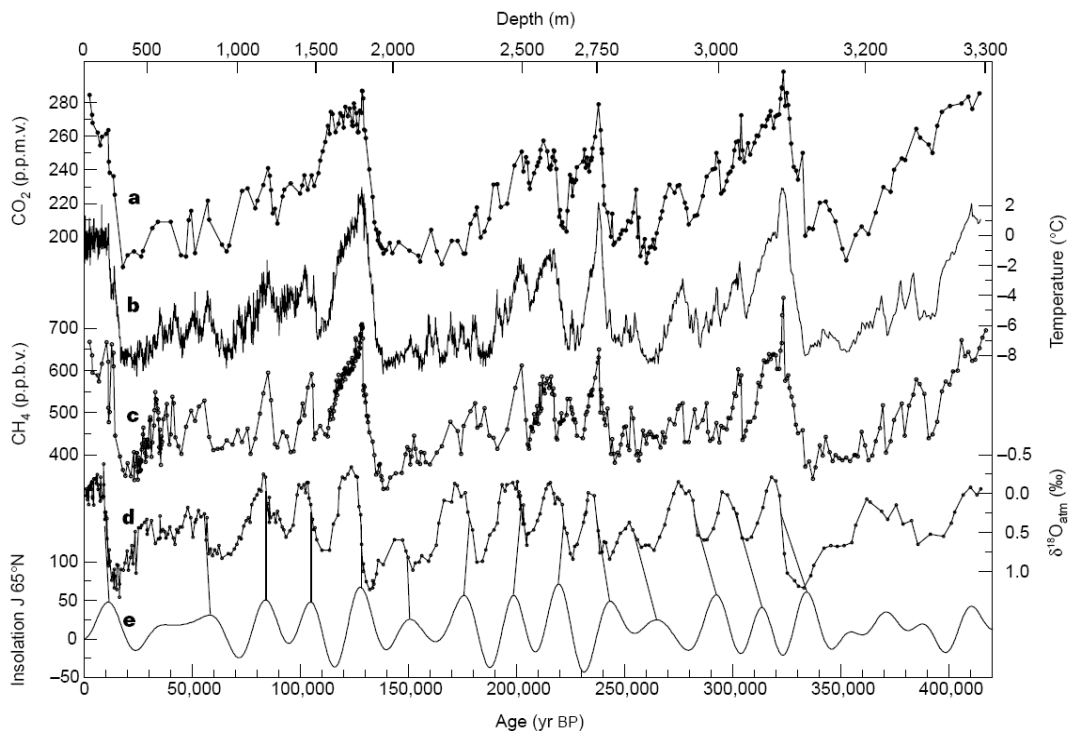


Figure 2: Vostok time series with temperature and insolation
From (Petit et al. 1999)

The Vostok temperature and ice volume plots clearly depict the four glacial-interglacial cycles. Figure 2 shows insolation, the solar radiation at the earth's surface, and its phase relative to atmospheric oxygen-18 ($\delta^{18}\text{O}_{\text{atm}}$). Figure 2 also shows the direct relationship of carbon dioxide (CO_2) and methane (CH_4) with temperature. What is hard to see in this plot is that the extension of present-day levels of CO_2 and CH_4 (~360 parts per million by volume (ppmv), and ~1,700 parts per billion by volume (ppbv), respectively) are unprecedented during the past 420,000 years. Details and further explanations can be found in (Petit et al., 1999).

The latest cores comes from the European Project for Ice Coring in Antarctica (EPICA), go back ~720,000 years, and reveal eight glacial cycles (Siegenthaler et al., 2005).

Climate Forcing

The climate system is in a state of transient planetary energy balance (McGuffie & Henderson-Sellers, 2005), responding dynamically fluxes of energy from both external and internal sources, causing changes in global temperature. Forcing is an imposed change to this balance and comes in two distinct categories, external and internal. External forcing is from causes outside the climate system and is usually due to variations in received solar radiation (*insolation*), while internal forcing is caused by changes within the system itself, such as volcanic eruptions, land-use changes (deforestation), ice-sheet changes, changes in atmospheric CO_2 (and other greenhouse gas) concentration, and in the long-term, changes in ocean currents and continental drift.

External Forcing Factors

Milankovitch Cycles

Also known as the Milankovitch theory, named after Milutin Milankovitch, a Serbian mathematician who correlated past glaciations (ice ages) with changes in insolation due to the following three changes in the earth's orbit.

- *Eccentricity* is the variation of earth's solar orbit from more eccentric or elliptical (less incident flux) to more circular (greater flux) with a periodicity of ~100,000 years.
- *Obliquity* or *Axial Tilt* is the variability (22° to 24.5°) in the angle of tilt of the earth's axis of rotation with the ecliptic (the plane of planetary rotation around the sun). The total received radiation is not affected but the range of seasonal variation increases directly with the angle. The periodicity is ~40,000 years.
- *Precession* is the slow "wobble" of the earth's rotational axis and movement of the orbital ellipse around in space due to gravitational interaction with other planets, primarily Jupiter. This causes a progressive change in the time of the equinoxes. Currently, perihelion (where the earth's eccentric orbit is closest to the sun) is on the 5th of January, but in ~11,000 to 15,000 years it will be in July. Like for obliquity, this will not affect the total radiation received, but will affect its temporal and spatial distribution. When the aphelion (orbital point furthest from the sun) occurs in winter and perihelion in the summer, it is believed that in the

Northern Hemisphere the winters will be colder and the summers hotter.

There are two periodicities of ~23,000 and ~18,800 years.

The Vostok deuterium (proxy for temperature) power spectrum (Figure 3 below) shows periodicity in agreement with the Milankovitch theory with spikes at 100 kyr (for eccentricity), at 41 kyr (for obliquity) and 23 & 19 kyr (for precession).

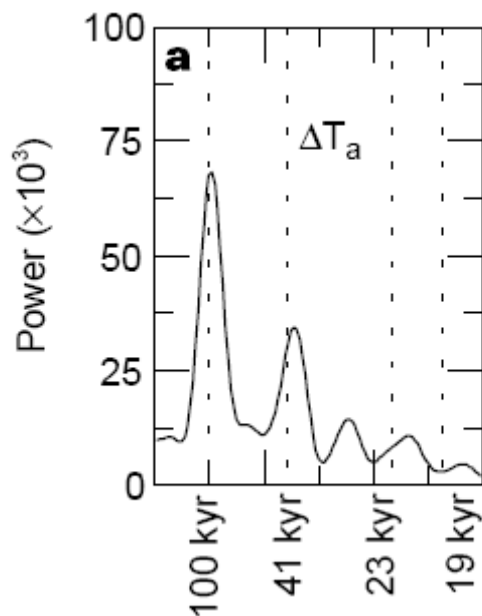


Figure 3: Vostok temperature (deuterium) power spectrum
From (Petit et al. 1999)

Solar Radiation Variability

Sunspot cycles have been linked to historical variations in climate. The *Hale* double sunspot cycle occurs with a 22 year periodicity with overall amplitude of cycles slowly increasing and rapidly falling with a period of 80 to 100 years. There has also been observed a quasi-cyclic fluctuation of 180 years. Correlation between sunspot activity and global surface

conditions has not yet been demonstrated. It is believed that forcing from sunspots is overwhelmed by other factors such as greenhouse gasses (McGuffie & Henderson-Sellers, 2005).

Comets and Large Meteors

Collisions with comets and large meteoric impacts have also been proposed as causes of variations in climate (McGuffie & Henderson-Sellers, 2005). The resulting disturbances of these events, such as an increase in atmospheric aerosols, is very similar to internal factors, both natural and human-induced, that it is hard to differentiate them. A recent theory proposes that an impact from an asteroid, the *Younger Dryas Impact event*, triggered the Younger Dryas abrupt climate change (Kerr, 2007).

Internal Forcing

Internal climate forcing is considered to come from both natural and anthropogenic (human-induced) causes.

Atmospheric Composition

Carbon Dioxide (CO₂), methane (CH₄) and nitrous oxide (N₂O) are known as the *greenhouse gasses* primarily because of their ability to produce a global greenhouse effect, trapping heat in the earth's atmosphere by inhibiting its radiation into space. The primary source of increased atmospheric concentration of CO₂ is anthropogenic due primarily to fossil fuel use

and to a smaller extent, land use change (Intergovernmental Panel on Climate Change, 2007a).

As the primary greenhouse gas implicated in global warming, CO₂ concentration in the atmosphere was measured at 379 ppm (parts per million) in 2005 which exceeded the natural range of 180 to 300 ppm over the last 650,000 years (from ice core data). Methane and nitrous oxide concentrations have also increased due to fossil fuel use (methane) and increased agricultural land use (methane and nitrous oxide) to levels exceeding pre-industrial values. 2005 levels of methane at 1774 ppb (parts per billion) far exceeds the 650,000 ice core range of 320 to 790 ppb, and 2005 nitrous oxide levels at 319 exceeds the pre-industrial level of 270 ppb.

Tropospheric and stratospheric aerosols are also recognized as having an effect on the climate. Volcanic aerosols (ash, cinders, and sulfate particles from SO₂ oxidation) have long been recognized as affecting climate. The eruptions of Mount Tambora in 1815 and Krakatoa in 1883 reduced global temperatures for several years. Anthropogenic contribution of carbon and sulfate particles as by-products of fossil fuel and biomass burning have contributed to a phenomena know as *global dimming*, where aerosol particles in the atmosphere tend to reflect more solar radiation back into space.

Destruction of stratospheric ozone has also been attributed to anthropogenic contribution of chlorofluorocarbons (CFCs) and hydrochlorofluorocarbons (HCFCs). This has moderated as a result of the Vienna Convention and the Montreal Protocol and with the substitution of hydrofluorocarbons (HFCs) for the offending gasses. All of these gasses are also more radiative (more effective greenhouse gasses) than CO₂, and therefore also contribute to global warming.

Land-use Changes

Desertification, deforestation, agriculture, urbanization, dams and huge water-works projects are some of the human endeavors that alter the character of the earth's surface. All of these force changes in albedo (reflection of solar radiation – see Figure 4 below for indices of various surface conditions), hydrological cycles (atmospheric-terrestrial water exchange), and biochemical (plant CO₂ - O₂) exchange as well as other processes that effect the global climate (McGuffie & Henderson-Sellers, 2005).

Ice

The extent global surface ice and snow cover has a direct relationship with albedo, the index of solar reflectivity. With greater the surface coverage of ice and snow, more radiation is reflected into space, with lesser coverage, more heat is absorbed. Figure 4, below, shows the reflectivity for various surface conditions.

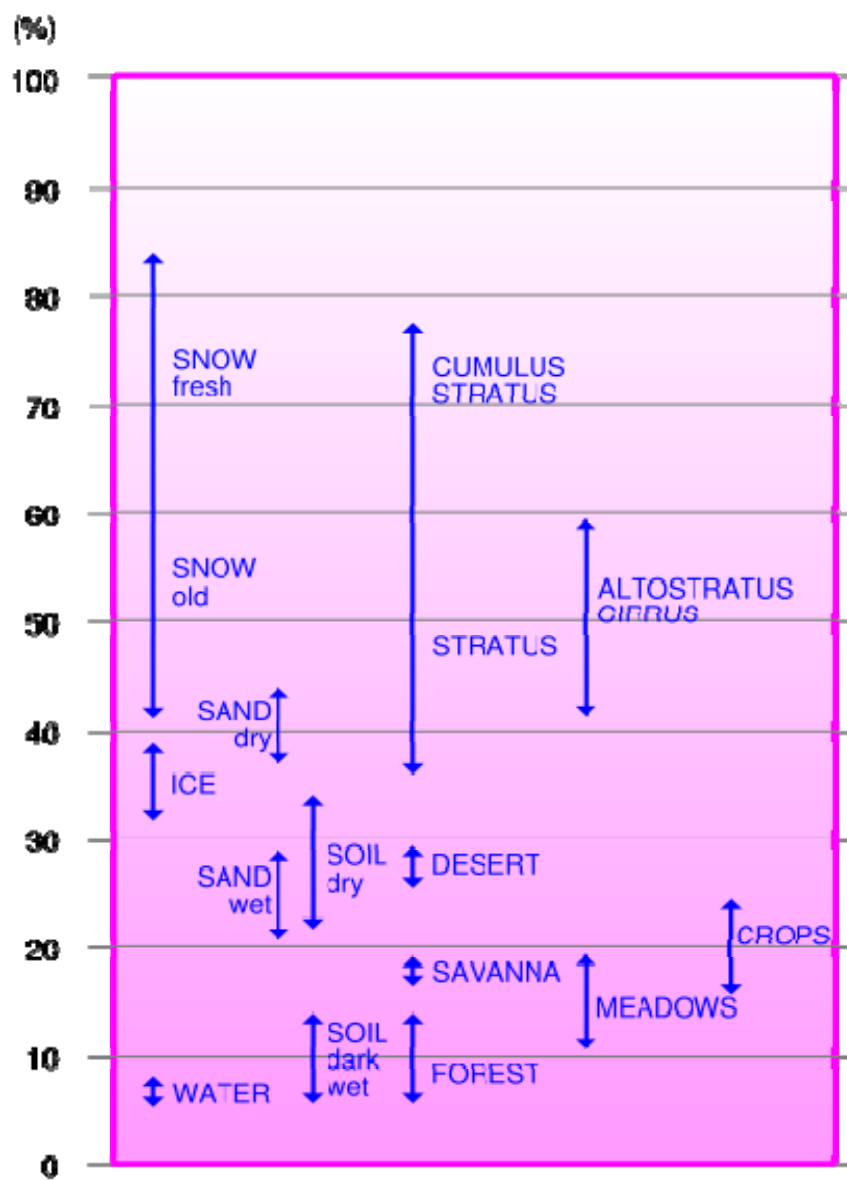


Figure 4: Albedo: percentage of reflected sunlight for various surface conditions
 From (<http://en.wikipedia.org/wiki/Albedo>)

Ocean Currents

The sheer size of the world ocean (71% of the earth's surface) makes it a main constituent and forcing factor of the climate system. Due to its size, the ocean absorbs most of the solar radiation received at the earth's surface which warms the surface waters. With the heat capacity of water and circulation, the ocean is able to store and redistribute the absorbed heat before releasing it to the atmosphere in the form of water vapor or radiating it back into space (Rahmstorf, 2002). Large scale ocean circulation is a combination of currents driven by winds, tides, and fluxes of heat and freshwater on the surface with subsequent interior mixing of heat and salt (thermohaline). A simplified depiction of global ocean currents is shown in Figure 4 below.

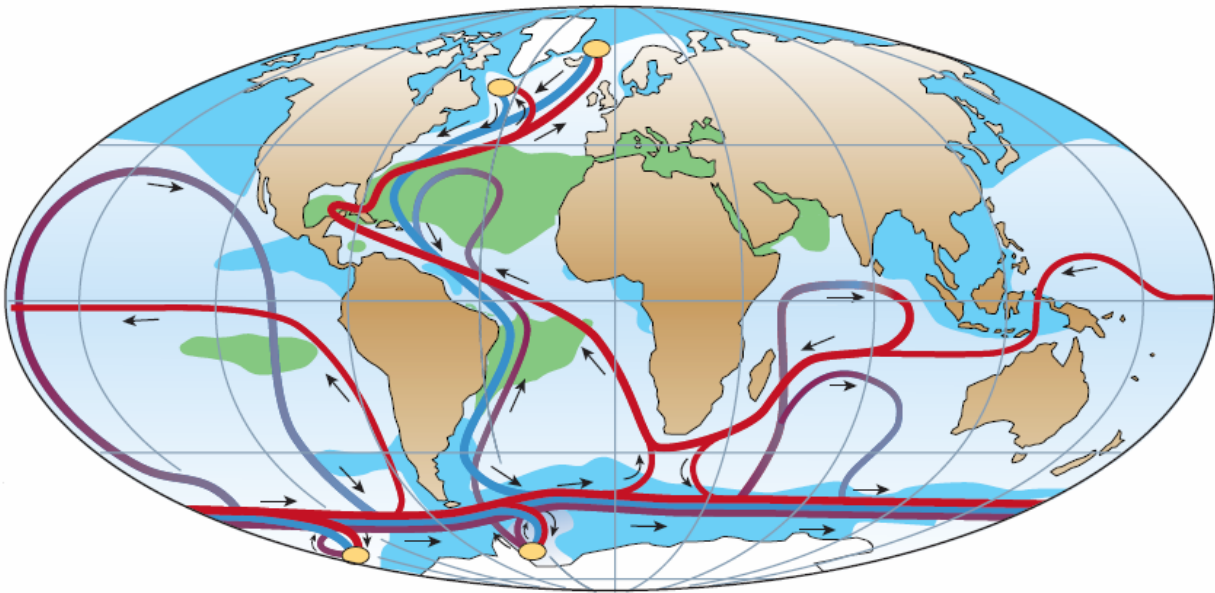


Figure 5: Global Ocean Circulation

From (Rahmstorf 2002): Red: near surface flows towards Yellow Ovals: deep water formation regions
Blue: deep currents, Purple: bottom currents, Green shading: salinity >36%, Blue shading: salinity <34%

(Rahmstorf, 2002) suggests that three different circulation modes have existed in the past (Figure 5); the stadial (cold), interstadial (warm) and Heinrich (off) modes. In the interstadial (warm phase within a glacial period), North Atlantic Deep Water (NADW) formed in the Nordic Seas (further north); in the stadial (cool phase within an interglacial period), it formed in the subpolar North Atlantic (south of Iceland), and in the Heinrich mode, NADW formation just about shut down with deep waters from the Antarctic filling the Atlantic basin. Heinrich events were stadial, with massive amounts of icebergs breaking loose from the Laurentide ice sheet and traversing the North Atlantic toward Europe. The prodigious amount of freshwater from the melting icebergs is believed to have disrupted or shut down the thermohaline circulation. Four to six Heinrich events have been identified from sediment deposits on the ocean bottom.

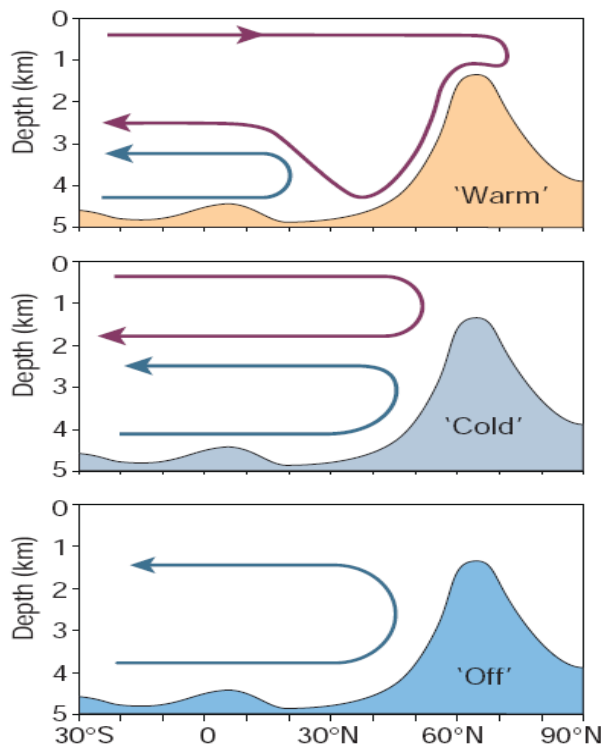


Figure 6: Three North Atlantic Glacial Ocean Circulation Modes

From (Rahmstorf 2002): cross-section of the North Atlantic with rise in bottom topography symbolizing the sill between Greenland and Scotland. Red line: North Atlantic overturning (NADW), Blue line: Antarctic bottom water

Dansgaard-Oeschger (D-O) events are perhaps the most pronounced abrupt climate fluctuations during the last 120k years (last glacial cycle). Twenty-three have been identified from ~110k to 23k years BP. D-O events are fairly large in amplitude, with rapid warming, typically over a few decades, and a much more gradual cooling. Global isotope data has revealed that D-O amplitudes were greatest in the North Atlantic with Southern Hemisphere, especially South Atlantic, sites showing a “see-saw” pattern of warming while the north was cooling. D-O and Heinrich events are related in that each Heinrich event is followed by a particularly warm D-O event with successive D-O events (without preceding Heinrich events), separated by approximately 1,500 years (3k year cycle), becoming progressively cooler until the next Heinrich event. This has sometimes been called the Bond cycle and may be attributed to the Laurentide ice sheet growing gradually between Heinrich events. It is believed that the thermohaline circulation played a significant role in the D-O events, but several different theories have been proposed on the mechanics. (Rahmstorf, 2002) proposes that the rapid warming phase results from the northward intrusion of warm Atlantic waters into the Nordic Seas (interstadial/warm phase) which eventually, over several centuries, weakens to the cooling (stadial) phase. The trigger for these events is still not clearly understood.

At approximately 12,700 year BP, the last D-O event gave way to the Younger Dryas cold event (stadial) that is believed to have shut down NADW formation (thermohaline circulation). NADW shutdown has been attributed to the emptying of Lake Agassiz, a massive North American freshwater lake formed by glacial melt, into the North Atlantic via the St. Lawrence River, or by a freshwater pulse ~1,800 year earlier (Sima, Paul & Schulz, 2004). It lasted until 11,500 years BP, giving way to a warming event similar to a D-O event (3k year cycle). Unique to the Younger Dryas are the rapid transitions, both cooling and warming, that

lasted only several decades. This warming was followed with a strong freshwater pulse, except that the Atlantic circulation remained in the warm mode into the Holocene. Global isotope data shows that the Younger-Dryas was a global cooling event, not a see-saw pattern, with a re-advance of ice in both hemispheres (some data dating places the Southern Hemisphere cooling ahead of the Northern Hemisphere by ~1,000 years), and because of this, it is believed that the Younger Dryas was a result of multiple causes, not just a change in ocean currents. As stated earlier, a recent theory proposes that the Younger Dryas was triggered by impact from an asteroid (Kerr, 2007).

Present-day climate/ocean-current research is focusing on the El Niño/Southern Oscillation (ENSO) as a strong mode of climate variability. Coral data have shown that ENSO was evident in glacial and interglacial times, with the strongest ENSO in modern times. At this time, more information (data, simulations with better models, etc.) is still needed to understand the role of ENSO variations through time. What climate study has shown, is that the “climate system is sensitive to forcing, and the role of the ocean is that of a highly non-linear amplifier of climatic changes (Rahmstorf, 2002).”

Teleconnections

The concept of *Teleconnections* is important in the development of climate hypotheses as well as climate models. Global climate events showing correlation are considered to be teleconnected. The American Meteorological Society (AMS) defines teleconnections as:

- A linkage between weather changes occurring in widely separated regions of the globe.

- A significant positive or negative correlation in the fluctuations of a field at widely separated points. Most commonly applied to variability on monthly and longer timescales, the name refers to the fact that such correlation suggest that information is propagating between the distant points through the atmosphere.

Teleconnections believed to be strongly correlated to TC activity are the *El Niño (La Niña) / Southern Oscillation (ENSO)* and the *Thermohaline Circulation (THC) / Meridional Overturning Current (MOC)*.

El Niño (La Niña) / Southern Oscillation (ENSO)

ENSO is a disruption of the ocean atmosphere system in the tropical Pacific evidenced by a relaxation of easterly trade winds and warmer SSTs in the eastern Pacific. La Niña is the opposite with cooler SSTs in the eastern Pacific that extend further west than normal. Central and eastern equatorial Pacific Ocean SST variations associated with ENSO and monsoon rainfall in Africa's Sahel region have been correlated (teleconnected) with variation in Atlantic hurricane activity. Warm phase ENSO (El Niño) is linked with increased shear in the Atlantic MDR resulting in less active seasons while cool phase ENSO (La Niña) is linked to less shear in the MDR with more active Atlantic hurricane seasons (Gray, 1984). Global Circulation Models have been run to simulate the correlation of ENSO with TC activity (Wu & Lau, 1991). ENSO periodicity has historically been decadal (10 to 15 yrs.), but recent activity records have shown shorter (4 yr.) periodicity.

Thermohaline Circulation (THC) and Meridional Overturning Current (MOC)

The THC refers to the Atlantic “heat conveyor” which includes the *Gulf Stream*. THC describes the transport of saltier and denser (due to evaporation) tropical Atlantic surface water to higher latitudes where it is eventually cooled and being denser sinks (Rahmstorf, 2002). This only happens in the north Atlantic, just east and south of Greenland, and not in the Pacific. The circulation takes the cooled, denser water throughout the world oceans, including the south Atlantic, Pacific, Indian and Southern Oceans before warming and returning to the surface. It is believed to take up to 1000 years. The MOC is a more general term that refers to the global circulation of surface and deep water currents and is often used synonymously with THC. Measurement of the flows at different depths across the full width of the Atlantic is used to gauge the strength of the THC/MOC.

As a heat transporter or “conveyor belt,” the THC is closely related to both the AMO and NAO, distributes thermal energy throughout the world and is believed to be the cause of Europe’s mild climate despite Europe’s high latitude. In the last decade, hurricane forecasters have felt that the THC was a major factor in determining TC activity (Gray & Klotzbach, 2005). The problem was, it was hard to determine its strength and nobody was sure what role it played. Forecaster in the early 1990s believed that the THC was strong, moved heat further north, decreased vertical shear in the MDR, thereby contributing to increased TC activity (Gray & Klotzbach, 2005). Other recent research (Hakkinen & Rhines, 2004) (Bryden et al., 2005) is suggesting that the THC may actually have been slowing, especially in the last decade, and if true, would not correlate positively with the recent increase in TC activity.

Satellite studies (Hansen, 2006) of the Greenland ice cap show that it is melting at twice the rate of five years ago, much faster than scientists had expected. High-latitude rainfall and accelerated polar and glacial ice-melt, due to climate warming and increased humidity levels is providing an infusion of freshwater into the world's polar oceans. This threatens to raise global sea levels and to disrupt the THC by diluting the denser surface water transported from the tropics thus slowing down the THC by inhibiting dense-water sinking. As mentioned above, some researchers feel that this is already happening. A complete collapse of the THC is considered a low-risk, high-impact event, meaning that the risk of a complete shutdown is considered unlikely, but the impact to the world's climate could be very high.

The affect of THC variability on TC activity is not yet well understood. As stated above, some hurricane researchers and forecasters felt that the THC was in a strong phase and contributed to increased TC activity (Gray & Klotzbach, 2005), while others have shown that the MOC (and by association, the THC) has weakened by approximately 30% in the last decade or so (Bryden et al., 2005).

Related Teleconnections

Other climate and weather patterns that have shown correlation or teleconnection to ENSO, THC/MOC and TC activity are the NAO, AMO, PDO, and MJO, described below.

North Atlantic Oscillation (NAO)

The NAO is a coherent seesaw pattern in sea-level air pressures (SLPs) between the Azores and Iceland. The NAO Index (NAOI) is a normalized pressure difference between them.

A positive index indicates a strengthening North Atlantic (NA) subtropical high-pressure area that shifts eastwards, allowing hurricanes along the U.S. east coast to re-curve to the east and posing a greater threat to the northeast (New England, Canadian Maritimes). Negative NAOI values indicate a weakening and westerly shift of the NA subtropical high pressure, steering hurricanes south and threatening the southeast U.S coast and the Gulf of Mexico. NAO periodicity approximately 8 to 10 years and some believe that it is tied to 11-year solar activity cycles.

Atlantic Multidecadal Oscillation (AMO)

The AMO is an ongoing series of long duration changes in north Atlantic SSTs. The AMO affects northern hemisphere rainfall variability and north Atlantic TC activity. Warm phases tend to create and exacerbate droughts in the mid and southwestern U.S., produce greater rainfalls in the Pacific Northwest and Florida, and produce more severe north Atlantic hurricane activity. AMO is also believed to mask the changes due to anthropogenic emissions (global warming) as AMO variability is considered greater. We are considered to be in a warm-phase AMO that has a multidecadal periodicity (20 to 40 yrs.).

Pacific Decadal Oscillation (PDO)

The PDO is a long-lived ENSO-like pattern of Pacific climate variability. PDO has warm and cool phases with extremes marked by widespread variations in Pacific Basin and North American climate. The PDO signature is most prevalent in the North Pacific and North American areas while ENSO is prevalent in the Pacific tropics. PDO and ENSO are usually

grouped for climate predictions but do have individual signatures. PDO, at this point, is not as well known or studied as ENSO. PDO persistence or periodicity is 20 to years.

Madden-Julian Oscillation (MJO)

The MJO is an eastward progression of large regions of both enhanced and suppressed tropical rainfall, affecting mainly the Indian and Pacific Oceans, but has also been observed in the tropical Atlantic. MJO phases have also been correlated to variations in TC activity. The MJO is considered intra-seasonal with cycles lasting approximately 30 to 60 days.

Tropical Cyclone Genesis

William Gray was one of the first researchers to present an observational study (Gray, 1968) of the atmospheric conditions associated with tropical disturbances and storm development. He identified the development regions as well as the correlation of TC development with warm sea surface temperatures (SSTs) and low vertical wind shear. Gray developed this further (Gray, 1979) with a statistical study of global tropical cyclone genesis frequency and its relationship to specific climatological parameters such as global moisture and kinetic energy budgets. These studies provided a foundation for a lot of subsequent TC research, much of which he also participated in.

Based on these studies, it is assumed that the greater TC activity since 1995 can be attributed to simultaneous increases in sea-surface temperatures (SST) and decreases in vertical wind shear. It is also believed that these changes exhibit fluctuations on a multi-decadal time scale and that the present cycle of high Atlantic hurricane activity may persist for a ~10 to 40 year period

(Goldenberg et al., 2001). The previous cycle of higher activity was observed from the late 1920s through the 1960s. A resurgence of higher activity occurred in 1988 and 1989, but returned to lower levels from 1991 to 1994. This suppression of activity has been attributed to a long lasting ENSO/El Niño event (1990 to 1995).

Looking at long-term variability requires looking at the oceans, as they are the primary energy source for TC. Warmer SSTs provide increased water vapor and decrease atmospheric stability that contributes to TC formation. SSTs greater than 26.5° C are considered a necessary condition for TC development, with higher SSTs positively correlating with increased major TC activity.

A dominant factor for TC development is the magnitude of the vertical shear of the horizontal wind between the upper and lower troposphere. Strong shear prevents the formation and intensification of TCs by inhibiting the axisymmetric organization of deep convection. It appears (Goldenberg et al., 2001) that reduced shear corresponds to warmer SSTs, especially in the Atlantic hurricane *main development region* (MDR - 10° to 14° N, 20° to 70° W).

Anthropogenic Global Warming

The anthropogenic (human-induced) contribution to the rise in atmospheric concentrations of greenhouse gasses (carbon dioxide (CO_2), methane (CH_4), nitrous oxide (N_2O), etc.) is well documented (Center for Global Environment, 2004) and accepted in the scientific community. The atmospheric level of CO_2 , for example, has risen ~25% to 32% over pre-industrial levels and is expected to double in the next 70 years. What lacks consensus is the

effect these elevated levels of greenhouse gasses will have on the earth's climate and the link to TC activity.

Until recently, it was believed that the seasonal and multi-decadal variations in climate and TC activity are much greater than the anticipated small climatic changes resulting from increased atmospheric levels of greenhouse gasses that any signal of anthropogenic climate change would be hard to impossible to detect and validate. This viewpoint is being modified towards one of greater anthropogenic causality as more observations and data are collected.

According to (Center for Global Environment, 2004):

- Atmospheric composition is changing (increasing levels of greenhouse gasses due to human activities)
- Global temperature is increasing
- SST is rising globally ($\sim 1^\circ$ F in the 20th century)
- Deep oceans are warming throughout the world
- Polar ice is retreating/melting
- Low latitude surface water is becoming more saline (increased evaporation) and water masses at high latitudes have become fresher (less saline due increased precipitation and glacial melt, possibly influencing thermohaline circulation)
- Atmospheric water vapor content is increasing (empirical evidence shows that atmospheric water vapor in the atmosphere increases $\sim 7\%$ - 10% for every 1° C ($\sim 2^\circ$ F) SST increase)
- Increased SST and atmospheric water vapor provide greater fuel for TC development

- Global sea level has risen about 1.25 inches in the last ten years (mostly due to thermal expansion and 20% to 35% from glacial melt)
- Surface pressures and winds are affected creating dramatic swings and extremes in climate (more variance and variability, more outliers, less stability)
- We are now seeing or considering much more likely and more rapid climatic changes of high consequence that were considered unlikely in the near future only half a decade ago, such as:
 - The rate of ice loss in Greenland
 - Loss of Antarctic ice sheets
 - Changes in ocean circulation
 - The need of biological and socio-economic adaptation to more rapidly changing climate

Intergovernmental Panel on Climate Change (IPCC)

The *Intergovernmental Panel on Climate Change* ([IPCC](#)) was established in 1988 by the United Nations' *World Meteorological Organization* (WMO) and the *United Nations Environment Programme* (UNEP) to assess scientific, technical, social and economic information relevant to human-induced climate change, its potential impacts as well as options for adaptation and mitigation. The IPCC does not perform any research but bases its assessments reports on peer-reviewed and published scientific and technical literature. Assessment reports are issued on a 5 to 6 year cycle with reports issued in 1990, 1995, 2001, and 2007. The 2001 report is generally referred to as TAR (*Third Assessment Report*), and the 2007 report as AR4 (*Fourth*

Assessment Report). AR4, like previous assessment reports, consists of four reports, three of them from working groups. *Working Group I* (WGI) dealt with “*Physical Science Basis of Climate Change*,” *Working Group II* (WGII) with “*Climate Change Impacts, Adaptation and Vulnerability*,” and *Working group III* (WGIII) with “*Mitigation of Climate Change*.”

The AR4 WGI report (Intergovernmental Panel on Climate Change, 2007a), looking at past climate as well as projections based on simulations from a broad range of models, makes the following observations and quantitative estimates of future changes.

- “The linear warming trend for the past 50 years is twice that of the past 100 years, and that most of the increase in the last 50 years is *very likely* (> 90% probability) to the observed increase in anthropogenic (human-caused) greenhouse gas concentrations.”
- “Warming of the climate system is unequivocal, as is now evident from observations of increases in global average temperatures, widespread melting of snow and ice, and rising global average sea level.”
- “Paleoclimate information supports the interpretation that the warmth of the last half century is unusual in at least the previous 1300 years. The last time the polar regions were significantly warmer for an extended period (about 125,000 years ago), reductions in polar ice volume led to 4 to 6 meters of sea level rise.”
- “Global atmospheric concentrations of carbon dioxide, methane and nitrous oxide have increased markedly as a result of human activities since 1750 and far exceed pre-industrial values determined from ice cores spanning many thousands of years. The global increases in carbon dioxide concentrations are due primarily to

fossil fuel use and land-use change, while those of methane and nitrous oxide are primarily due to agriculture.”

- “At continental, regional, and ocean basin scales, numerous long-term changes in climate have been observed. These include changes in Arctic temperatures and ice, widespread changes in precipitation amounts, ocean salinity, wind patterns and aspects of extreme weather including droughts, heavy precipitation, heat waves and the intensity of tropical cyclones.”
- “Continued greenhouse gas emissions at or above current rates would cause further warming and induce many changes in the global climate system during the 21st century that would *very likely* be larger than those observed during the 20th century.”
- “Model experiments show that even if all radiative forcing agents are held constant at 2000 year levels, a further warming trend would occur in the next two decades at a rate of 0.1°C per decade, due mainly to the slow response of oceans.”
- Temperatures and sea-levels are projected to rise (warming reduces CO₂ uptake)
- Snow cover projected to contract, with widespread increases in permafrost thaw depth
- Sea ice is projected to shrink in both the Arctic and Antarctic. In some projections, Arctic late-summer ice disappears almost entirely by the end of the 21st century
- It is *very likely* that hot extremes, heat waves, and heavy precipitation events will become more frequent

- It is *likely* (> 66%) that future tropical cyclones will become more intense with larger peak wind speeds and more heavy precipitation associated with increases in tropical SSTs
- Extra-tropical storm tracks are projected to move poleward, with consequent changes in wind, precipitation and temperature patterns, continuing observed trends over the last half-century
- Increases in the amount of precipitation are *very likely* in high-latitudes, while decreases are *likely* in most sub-tropical land regions
- It is *very likely* that the meridional overturning current (MOC/THC) of the Atlantic Ocean will slow down during the 21st century, with multi-model average reduction of 25% by 2100 (some current research (Bryden et al., 2005) suggests the MOC has already been reduced by approximately 30%)
- Temperatures in the Atlantic region are still expected to increase, despite the projected decrease in the MOC/THC surface “thermal transporter” due to anthropogenic emissions
- It is *very unlikely* (< 10%) that the MOC will undergo a large abrupt transition (i.e., shutdown) during the 21st century, but longer-term changes cannot be assessed with any confidence

Links to Tropical Cyclone Activity

While the debate continues on whether the recent climatic events are simply part of a natural, multi decadal variation or human induced, there is increasing evidence that it is a combination of both. The question now is how significant is the human contribution.

While there is overwhelming evidence that we are in an active TC cycle, researchers are in disagreement as to how unprecedented is the current activity level, and how significant, if at all, is the human contribution (Pielke, Landsea, Mayfield, Laver & Pasch, 2005). Part of the problem is the amount and quality of data available. Climate cycles can last many decades, but the technology of measurement, observation and data collection advances daily. Our present day ability with aircraft reconnaissance (since 1950s) and satellite observations (since 1980s) is quite different from 100 or more years ago when records may have been only anecdotal or based on ship's logs. Even in the last 55 years, data collection has evolved so much that some researchers (notably W. Gray) contend that is not correct to consider the recent hurricanes any more intense than those of the previous active cycle (1920s to 1960s) due to these differences (Klotzbach, 2006). Other researchers (Emanuel, 2005) (Webster, Holland, Curry & Chang, 2005) have made certain assumptions and "normalized" the observational data to be able to make reliable comparisons over larger time periods data and have concluded that the current active cycle is unprecedented and has a significant anthropogenic (human-induced) contribution. Climatological evidence from the previous ~120,000 years obtained from tree rings, ice cores, corals and sediments suggests that the global climate has gone through numerous warm and cold cycles lasting for thousands to tens of thousands years (Rahmstorf, 2002). Whether the current active

TC cycle is an example of natural variability, or the result of anthropogenic emissions, or both is currently unresolved.

It has been generally anticipated by some that the changes to the climate from global warming (and consequently on TC development) in the near-term would be very small and therefore its signal would not be discernable in the context of greater natural variability. Predictions for TC wind increase for increases in 1° C SST (the increase for the last century) varies from about 5% (Emanuel, 2005) to somewhat less (Knutson & Tuleya, 2004) based on atmospheric General Circulation Models (GCMs). At this level, it could mean many decades of continued global warming before a valid signature is identified.

Modeling Climate and TC Activity

The mitigation of TC affects depends on forecasting future events. In the short term, accurate predictions (forecasts) allow timely preparation, such as securing property and population evacuation to lessen negative impacts. In the long term, more accurate forecasts of trends would allow for planning such as construction standards, evacuation routes, zoning for population density, and even lifestyle changes to mitigate negative climate and TC effects.

Climate Models

A model is a representation or description of an object, system or concept. Numerical models of the climate system are essential in the exploration and formation of quantitative hypotheses about the dynamics of climate changes (Rahmstorf, 2002). Climate modeling is therefore an attempt to simulate climate system dynamics with numerical representations of the

physical, chemical, and biological processes that make up the system, and can range from simpler one-dimensional *energy-balance models* to complex, fully-coupled, *atmosphere-ocean-biomes general circulation models* (AOBGCMs) (McGuffie & Henderson-Sellers, 2005).

Energy Balance Models

Energy balance models (EBMs) are typically single-dimensional calculations of radiation flux at the earth's surface, with the dimension being latitude and surface temperature as the variable. They are used for basic determination of energy budgets and evaluation of more complex and realistic models. *Radiative-convective* (RC) models are also one-dimensional with altitude as the dimension. The emphasis of RC models is average global surface temperatures, but can also provide temperatures at other levels of the atmosphere.

Earth Models of Intermediate Complexity

Earth models of intermediate complexity (EMICs) are typically two-dimensional, combining the latitudinal and vertical dimensions of EBM and RC models (McGuffie & Henderson-Sellers, 2005). EMICs are capable of more realistic latitudinal energy transport. Early EMICs used empirical and theoretical methods, using statistics to characterize wind speed and direction, and eddy diffusion coefficients for energy transport. Because of this, they became known as *statistical-dynamical* (SD) models. These have been superseded by three-dimensional models, but the dimensionally constrained EMICs, without physical dimensions, have lately become more popular in applications simulating socio-economic climate change assessments.

General Circulation Models (GCMs)

Short and medium-term (1 to 10 days) weather prediction is typically done by numerical weather prediction (NWP) models, such as NAM(ETA), GFS, NOGAPS, WRF, and COAMPS. NWP models produce the weather forecasts found on TV and weather statements issued by the National Weather Service (NWS). General Circulations Models (GCMs), also known as global climate models, use the same mathematical equations as NWP models, but are designed to numerically simulate changes in climate that result from slow changes in boundary condition or physical parameters (such as greenhouse gas concentration). GCMs typically run for much longer periods of time than NWP, sometimes for many years on end. The accuracy of GCM forecasts for specific weather events (such as fronts and other disturbances) is comparable to NWP models, but all models err in this respect over longer time periods, and after approximately 2 weeks, are useless for weather prediction. GCMs are typically run long enough to gather sufficient data to quantify climate and climate changes statistically. GCMs lend themselves to research about global warming, global climate patterns, and tropical and extra-tropical disturbances.

State-of-the-art GCMs are coupled atmosphere-ocean models. They are able to dynamically and simultaneously (in parallel) simulate the interaction between fast-changing atmospheres and slower-changing oceans. GCMs can also be coupled to land surfaces and sea ice to present a more complete simulation of global climate. Atmospheric GCMs can be referred to as AGCMs, fully-coupled ocean-atmosphere GCMs as AOGCMs, and with the inclusion of biomes, AOBGCMs.

Two of the better-known GCMs are the Geophysics Fluid Dynamics Laboratory's (GFDL) models and the Community Climate System Model (CCSM). GFDL is a laboratory in the National Oceanic and Atmospheric Administration (NOAA) and the Office of Oceanic and Atmospheric Research (OAR). GFDL is located at Princeton University's Forrestal Campus. CCSM is a collaborative effort between academia and government and is located at the National Center for Atmospheric Research (NCAR) in Boulder, Colorado.

Regional and Hybrid Models

As climate modeling technology advances, so do the options available to climate modelers. Multi-use models such as the NCAR Weather Research & Forecast ([WRF](#)) Model can be used for real-time weather prediction as well as climate research. WRF is used by NOAA (NWS, NCEP) and the military for weather forecasting. It is also used by researchers to study climate. It comes with different dynamical cores (ARW & NMM), has a 3-dimensional variable data-assimilation (3DVAR) system that feeds back observational data during a model run for corrective parameterization. The model resolution can vary from meters to thousands of kilometers. It can run as either a regional or global model. WRF supports multiple *nesting*, where nested areas are downscaled to a finer resolution (spatial and/or temporal) with either one or two-way interchanges with the parent area. WRF is built with an object-oriented framework that supports modularity and integration with other systems.

Earth System Modeling Framework

The *Earth System Modeling Framework* ([ESMF](#)) is a collaboration to build a high-performance, flexible software infrastructure to increase ease of use, performance portability, interoperability, and reuse in climate, numerical weather prediction, data assimilation, and other earth science applications. Collaboration partners include NOAA (GFDL, NCEP), NCAR, NASA, DoD (NRL, AFWA, Army), and numerous universities. There are also efforts to converge WRF with ESMF (*Final Report of the Technical Workshop on WRF-ESMF Convergence*, 2006).

Program for Climate Model Diagnoses and Intercomparison

The *Program for Climate Diagnoses Model and Intercomparison* ([PCMDI](#)) was established in 1989 at the Lawrence Livermore National Laboratory to develop methods and tools for the diagnoses and intercomparison of general circulation models (GCMs) used to simulate global climate. As more complex GCMs are developed and used in the study of global climate change, their disagreements have become significant and not always well understood. The PCMDI project's mission is to account for these differences and biases in a systematic way. Projects underway at PCMDI include the Atmospheric Model Intercomparison Project (AMIP), the Coupled Model Intercomparison Project (CMIP), the Seasonal Prediction Model Intercomparison Project (SMIP), the Aqua-Planet Experiment Project (APE), and the Paleoclimate Model Intercomparison Project (PMIP). PCMDI supports the work of the IPCC, providing storage and distribution of datasets used in the IPCC assessment reports.

Computational Resources for Climate Modeling

The size and complexity of climate models parallels developments in computational technology. The earlier one-dimensional energy balance models (EBMs) and radiative-convective (RC) models required relatively modest computational resources, at least when compared to the dimensionally-constrained (2-D) earth models of intermediate complexity (EMICs) and especially the three-dimensional, fully coupled atmosphere-ocean-biomes general circulation models (AOBGCMs).

Temporal and Spatial Factors

Each variable for each point in time and geographic position requires calculations and storage. Paleoclimate simulations that can span hundreds to thousands of years will typically have daily or monthly time increment with a 2° to 4° (222 to 444 km) spatial resolution, while the Weather Research & Forecast (WRF) model, which is used to simulate hurricanes, can have an hourly temporal and a 1 to 10 km spatial resolution. Coupled models add additional levels of complexity by running simultaneous simulations of the atmosphere, ocean, land, or whatever else is coupled. Generally, the longer the model run, and the finer the temporal and spatial resolutions are, the greater will be the computational (processing) and data storage requirements. While general computing performance is measured in *millions of instructions per second* (MIPS), processing for scientific (numerical) applications is measured in *floating point operations per second* (FLOPS). Using benchmarks like LINPACK or LAPACK, the general-purpose personal computer (PC) with an Intel Pentium-4 or AMD-64 is considered to be capable

of 10 gigaflops (GFLOPS) or 10×10^9 flops. The latest (and fastest), as of 2007, computer cluster is reported to be capable of 3 petaflops (PFLOPS) or 3×10^{15} flops.

Parallel Processing

Performance gains mentioned above are achieved primarily through parallel processing and not just processor improvements, although processor improvement itself is quite significant. Parallel or distributed processing is done with multiple processors (including multiple-core processors), also known as *nodes*. These can be multiple computers, multiple processors in one chassis, or any combination thereof. Table 3, below, provides a comparison of resolutions (T85 is the finest, and T35 is the coarsest resolution), model years, run time, and amount of processors used for the fully-coupled CCSM 3.0 AOGCM. It is interesting to note that the highest resolution (T85) required almost twice the number of processors to simulate the approximately the same amount to model years as the middle resolution (T42) in 24 hours, and it (T85) required three times the number of processors to simulate about 1/5 time done by the low resolution (T35) case in 24 hours.

The newest, as of this time, Department of Energy (DOE) super computer used for climate research is named *Jaguar* and has 10,400 processing cores, 21 terabytes (21×10^{12} bytes) of memory and is capable of 54 teraflops (TFLOPS) or 54×10^{12} (54 trillion) flops.

Table 3
CCSM 3.0 Resolution and Run Times

Resolutions (fully active)	Model Years	Run Time	<u>Performance</u>	
			Processors	NCAR Machines
T85_gxlv3	~4.5	24 hrs	192	bluesky
T42_gxlv3	~4	24 hrs	104	blackforest
T31_gxlv5	~24	24 hrs	64	bluesky

Information from NCAR CCSM 3.0 [FAQ](#)

Climate Data

Early climate modeling produced output that was fairly proprietary to the local system architecture and model used. Along with the development of UNIX and high-speed data communications (internet) came the need for data exchange and interoperability (McGuffie & Henderson-Sellers, 2005). Network common data form (netCDF) is a standard developed by the University Center for Atmospheric Research's (UCAR) [Unidata](#) program for data and data tools. Other gridded data file formats include HDF (see netCDF below), ASCII (text), and GRIB (1 & 2 - typically the formats used for real-time numerical weather forecast models).

Network Common Data Form (netCDF)

Network common data form (or format - [netCDF](#)) is a file standard developed for data interchange that is self-describing and machine-independent. It comes with a set of library functions that can be used to access the data and create new netCDF files. A set of utilities,

netCDF Operators (NCO) are command line programs that operate on netCDF files to derive new data, do averaging, hyperslab (create dimensional data subsets), manipulate metadata, and produce new netCDF files as output

Hierarchical Data Format (HDF) is a later scientific data format developed by UCAR's National Center for Supercomputing Applications ([NCSA](#)). It is similar netCDF in that it is also self-describing, machine-independent, and comes with a set of library functions. It is supposed to be more powerful and performance oriented, but it is not as popular or as wide-spread as netCDF. There are proposals to merge netCDF and HDF in the future.

Analysis and Visualization

Data analysis and visualization is an integral part of any research. Interpreted languages like Matlab, Python, and NCAR Command Language (NCL) along with programming languages like C, C++, and FORTRAN have been used in both modeling and analysis. Spreadsheets are also been useful for analysis and charting data that can input in text or certain database formats. The most useful utilities for manipulating and analyzing climate data are those developed specifically for those applications. NCAR Command Language ([NCL](#)) is a freely available, interpreted computer language designed for scientific data analysis and visualization, especially of climate data. It is available for different operating systems (Unix/Linux, Cygwin/Windows, MacOSX, etc.) and supports external routines in C, C++, and Fortran. NCL can read in netCDF/HDF, GRIB, ASCII, and IEEE binary files. It can also create output in netCDF/HDF, ASCII and IEEE binary files. NCL has over 600 functions and routines for climate data manipulation, analysis and visualization.

Another very useful climate data tool is PCMDI's *Climate Data Analysis Tools* ([CDAT](#)). It has capability similar to NCL, is freely available, is Python-based (interpreted language), and has an excellent *graphical user interface* (GUI), *Visual CDAT* (VCDAT), that NCL, at present lacks.

Tropical Storm Modeling

While relatively low-resolution GCMs are not adequate to forecast or simulate individual storms, they are useful for dynamical forecasts of seasonal tropical storm activity (Camargo & Sobel, 2003). Using GCMs to forecast tropical cyclone activity is usually done either of two ways. One way is to project large-scale and long-term changes in the variables affecting tropical cyclone activity. These parameters can then be used to parameterize another model, usually regional and/or with a finer resolution, to simulate a storm. This is particularly useful when studying the effects of long-term climate variation, such as global warming or change in ocean currents, on tropical storm activity. The other method is to detect and track tropical storms in the GCM output itself. The statistics obtained can reflect realistic spatial and temporal distribution (location and frequency) but not the intensity and size. The requirements to simulate long-term, large-scale events are quite different to simulating dynamic, relatively shorter-lived regional events such as tropical storms, which makes it difficult for any single model to do both. With ongoing developments in climate modeling, including global-regional models with nesting, hybrid models with physical-statistical components, along with advances in software architectures (ESMF) and computational capability (massive-parallel computing), the flexibility to realistically simulate more complex scenarios is increasing.

Tropical Cyclone-Like Vortices (TCLVs)

Currently, most climate forecasting requiring resolution of dynamic and non-linear systems is done with GCMs. Global climate is a dynamic process of interacting systems that can be described by relative pressures (high and low) and their associated flows and vorticity. Flows around high pressures (outflow) and low pressures (inflow) are characterized by cyclonic and anti-cyclonic vorticity, respectively. Extracting tropical cyclonic behavior requires identifying the characteristics of tropical cyclone-like vortices (TCLVs) that differentiate them from other vorticity. Wu and Lau (Wu & Lau, 1991) have proposed criteria in their study to identify TCLVs. The output data from the GFDL simulation in their study was analyzed daily. Meteorological fields examined include geopotential height at 200, 500 and 1000 millibars (mb), temperature and horizontal wind at 200 and 950 mb, water vapor mixing ratio at 950 mb, vertical velocity at 500 mb, and precipitation. The horizontal grid spacing used in their model data is 7.5° of longitude and 4.5° of latitude. The following criteria were used to identify cyclonic systems at grid point P in the zone bounded by latitudes 40.5° S and 40.5° N:

- At 1000 mb, the geopotential height at P must be at a minimum relative to the eight surrounding points.
- The 950 mb circulation at P must be both cyclonic and convergent.
- The thickness between 200 and 1000 mb over P must be at a maximum relative to the four neighboring points and must exceed, by 60 meters, the corresponding mean value of the grid points lying within 1500 km to the west and east.

- The wind speed at 950 mb must exceed gale-force strength (17.2 m/s) at one or more of the nine grid points in the proximity of P.

The systems satisfying these criteria are then classified as cyclones. As storm genesis was the purpose of the study and the data were analyzed daily, any cyclone identified a distance of 7.5° of longitude and 9° of latitude from a cyclone identified the previous day would be considered the same cyclone that has migrated and not counted as newly formed.

Analysis of the systems meeting the above criteria in the Wu and Lau study (Wu & Lau, 1991) included not only Tropical Storms, but also baroclinic (frontal) cyclones, continental dry cyclones, and equatorial easterly perturbations. To further isolate tropical systems, Wu and Lau added the additional constraints:

- The 200-mb zonal wind above the cyclone center P must not exceed 5 m/s (westerly).
- The 950-mb relative humidity at P must exceed 70%.
- The 950-mb zonal wind component must not be easterly at both the grid point located 4.5° to north and the point located 4.5° to the south of P.

Selection criteria for TCLVs were also developed in (Broccoli & Manabe, 1990) and are comparable to Wu and Lau's. They eliminated most baroclinic cyclones by considering only points up to $\sim 30^\circ$ either side of the equator and only during the 6-month warm TC season cycle. They also eliminated continental dry cyclones by considering only oceanic grid points. Both studies produced comparable results relative to TCLV detection.

A criticism of the Wu and Lau TCLV detection scheme for GCMs is that it is very similar to observed tropical storms (Vitart, Anderson & Stern, 1997). The realism of a modeled tropical storm or TCLV depends on model resolution and may also depend strongly on model

parameterization. This can cause the structure of simulated tropical storms to be very different from one GCM to another as criteria taken from observational values do not account for model biases. Subsequent and possibly more modern TCLV detection routines are based on closed pressure minima and thresholds for vorticity, upper level temperature anomalies (warm core) and winds. Details of these methods are detailed in (Vitart et al., 1997), (Nguyen & Walsh, 2001) and (Camargo & Zebiak, 2002).

(Camargo & Zebiak, 2002) outlines a methodology for tropical cyclone detection in low resolution atmospheric GCMs based on dynamical and thermodynamic values exceeding thresholds that are basin and model dependent. Using joint probability distribution functions (PDFs) of vorticity/temperature anomalies and vorticity/surface wind speeds, they develop basin-independent (Bind) and basin-dependent thresholds, shown in Table x below, for vorticity (ξ), surface wind-speed (v), and temperature anomalies (δT) for the North Atlantic (ATL), Eastern North Pacific (NP), Western North Pacific (WNP), South Pacific (SP), Australian (AUS), North Indian (NI), and South Indian (SI) basins in the ECHAM4.5 AGCM (T42: $2.8^\circ \times 2.8^\circ$). It is important to note that the threshold values for other models will probably be different.

Table 4
ECHM4.5 Basin Dependent & Independent TCLV Detection Thresholds

Parameter	Threshold Values							
	BInd	SI	AUS	SP	NI	WNP	ENP	ATL
$\xi \times 10^{-5}$	3.5	3.0	3.0	3.0	3.0	3.6	2.6	2.6
v (m/s)	15.0	11.4	11.8	11.2	12.0	11.8	10.4	10.4
δT ($^\circ\text{C}$)	3.0	2.1	2.0	2.1	1.7	1.9	1.9	1.9

From (Camargo & Zebiak 2006), For the ECHM4.5 vorticity (ξ), surface wind (v), and temperature anomaly (δT) thresholds

In (Camargo & Zebiak, 2002), details of the relative improvement of the basin-dependent (BInd) criteria over the absolute or basin-independent thresholds are presented. It is interesting to note in Table 4 that the values for the Atlantic basin (ATL) are lower than the other basins and that the surface wind velocity of 10.4 m/s is considerably lower than the observational value of 17 m/s for a tropical depression.

The criteria used in (Camargo & Zebiak, 2002) for TCLV detection is as follows.

1. The 850 hPa vorticity exceeds the vorticity threshold
2. The maximum surface windspeed in a centered 7×7 (grid point) box exceeds the windspeed threshold
3. The sea level pressure is the minimum in a centered 7×7 box
4. The local temperature anomaly averaged over the 7×7 box and the three levels: 300 hPa, 500 hPa, and 700 hPa exceeds the threshold
5. The local temperature anomaly at 300 hPa, 500 hPa, and 700 hPa are positive
6. The local temperature anomaly at 300 hPa is smaller than at 850 hPa
7. The mean speed averaged over a 7×7 box is larger at 850 hPa than at 300 hPa
8. The grid points representing the center of storms meeting the above criteria are connected (same storm) if in subsequent time steps they are no more than ~ 5.6 degrees apart in latitude and/or longitude (2 grid points for T42 resolution) for 6 hourly output or ~ 8.5 degrees (3 grid points) for daily output.
9. If the storm last for 1.5 days for 6 hourly output or 2 days for daily output, it is identified as a model tropical storm.

Freshwater Forcing

The role of ocean currents in climate change (Heinrich, Dansgaard-Oeschger, and Younger Dryas events) is being well researched and documented. An important mechanism in the variability of ocean currents is the dynamic of heat and salinity interaction that drives the thermohaline circulation (THC)/meridional overturning current (MOC). As described earlier, the cooling of relatively more saline (due to evaporation) and denser (due to increased salinity) tropical surface waters as they are transported poleward, especially in the North Atlantic, causes a further increase in density with subsequent sinking and overturning, which in the North Atlantic, forms the North Atlantic Deep Water (NADW) (Rahmstorf, 2002). A flux of surface freshwater in high latitudes, due to either glacial melt or precipitation, will dilute (reduce the salinity) of the poleward surface current, inhibiting the sinking/overturning mechanism. If the flux is great enough, it could shut down the overturning mechanism and formation of NADW, as is proposed to have happened during the Heinrich and Younger Dryas events (Rahmstorf, 2002).

(Stouffer et al., 2006) is a report on a set of coordinated experiments to study the dynamical behavior of the thermohaline circulation (THC) and THC-induced climate changes for the Program for Climate Model Diagnose and Intercomparison (PCMDI) Project's Coupled Model Intercomparison Project (CMIP) and Paleo-Modeling Intercomparison Project (PMIP). The experiments comprised of simulations of common design undertaken at institutions worldwide using their own coupled atmosphere-ocean general circulation models (AOGCMs) or earth models of intermediate complexity (EMICs). The AOGCMs are the main tools but require large

computer resources, so EMICs are also widely used. The experiments focused on in (Stouffer et al., 2006) are the so-called *water-hosing* experiments, where the response of the THC to an external freshwater source and the resulting changes in climate are studied.

In the experiment, three scenarios are run. There is a control scenario, where no additional freshwater is added, is based on 1860 (pre global-warming) conditions and is run for 200 years. In the first hosing scenario, an additional freshwater flux of 0.1 Sv (1 Sverdrup $\equiv 10^6 \text{ m}^3 \text{ s}^{-1}$) is added for the first 100 years uniformly in the North Atlantic between 50° and 70°N Latitude. After year 100, the freshwater flux is shut off and the model is run for an additional 100 years to simulate recovery. A freshwater flux of 0.1 Sv is approximately equal to the Amazon River runoff and is of the order of magnitude for a large CO₂-induced ($\sim 4 \times \text{CO}_2$) climate change.

Figure 6, below, shows the control run (no hosing) simulations of the different models used in the project. Even though the intensity levels are different, none of them show any trend of increase or decrease.

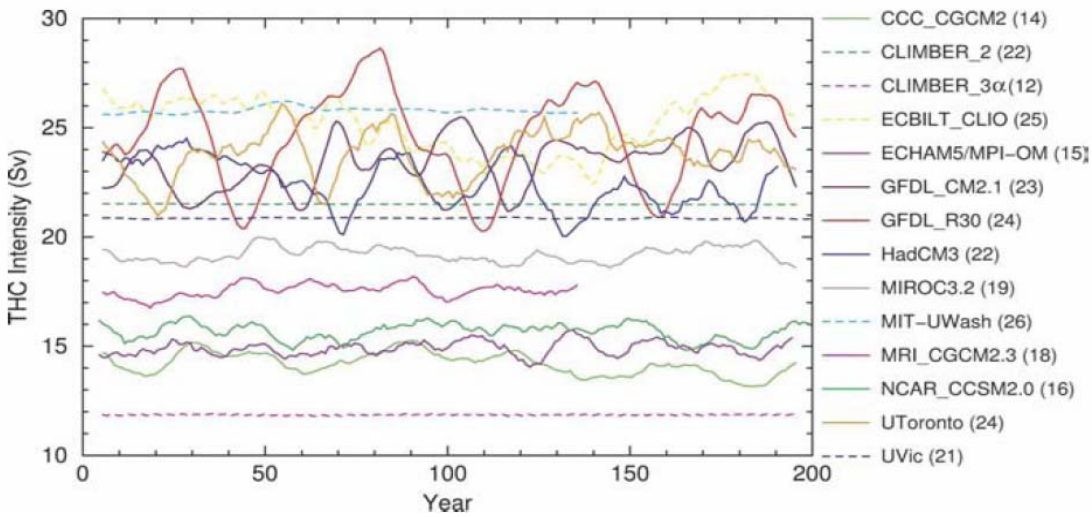


Figure 7: Time Series of THC Intensity (Sv) in Control Runs
 From (Stouffer et al. 2006): 10-year running mean (for smoothing)
 AOGCMs: Solid Curves, EMICs: Dashed Curves

Figure 8, below, shows the multi-model results from the 0.1 Sv hosing run. Figure 8a shows the absolute values from the different models, and figure 8b shows the relative values compared to the long-term mean of THC intensities from the control run. The black lines show the ensemble mean. All the models show a decline of THC intensity during the hosing period (1st 100 years) and a rebound when hosing is shut off (after year 100). Some of models show an overshoot with ringing (frequency fluctuations), but the ensemble mean shows a definite trend of THC intensity decline during hosing and a recovery after hosing is shut off. These results show that a freshwater flux of 0.1 Sv is not sufficient to shut the THC down. It is interesting to note that at the end of the model run (year 200) THC intensities for most models have not yet recovered to an equilibrium state.

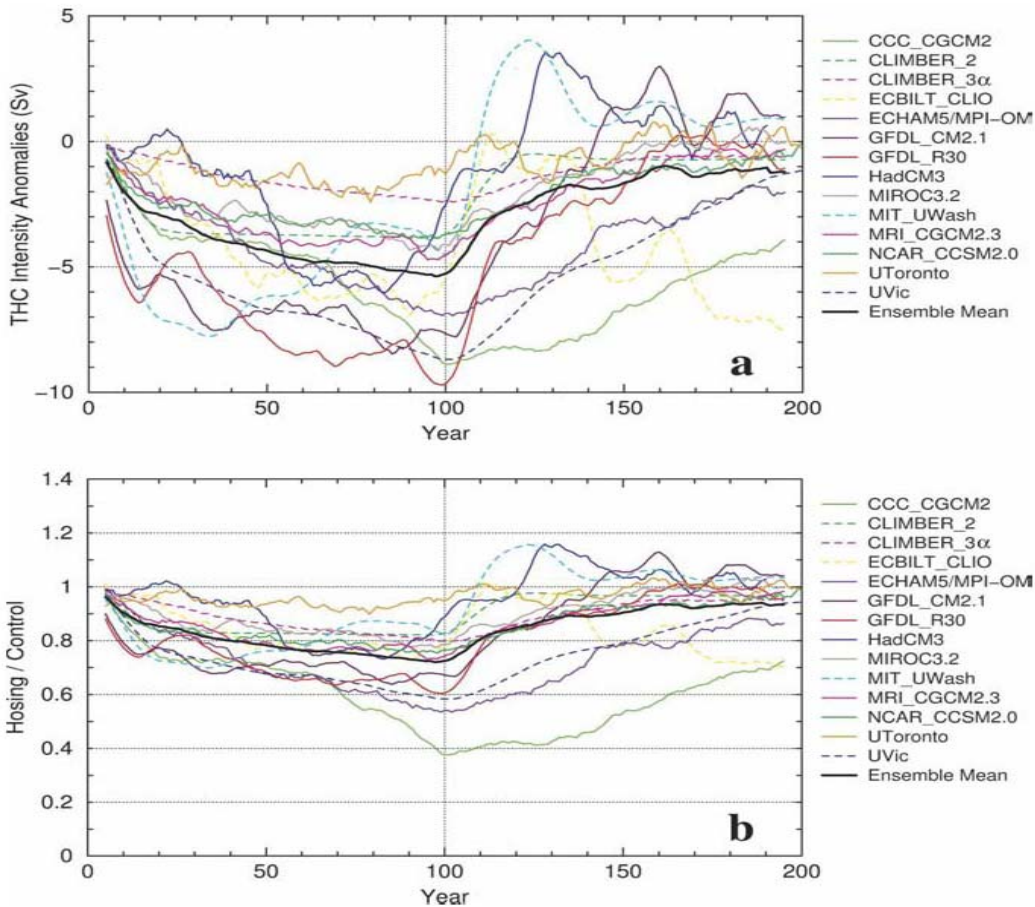


Figure 8: Time Series of THC Intensity (Sv) in 0.1 Sv Water-Hosing Runs
 From (Stouffer et al. 2006): (a) absolute values, (b) relative values to long-term control mean
 AOGCMs: Solid Curves, EMICs: Dashed Curves

Some of the models in the study also ran a 1.0 Sv scenario, with water-hosing for the first hundred years followed by 200 years of recovery. 1.0 Sv of freshwater flux is an order of magnitude greater ($10\times$) than the 0.1 Sv flux of the previous scenario. 1.0 Sv freshwater flux is equivalent to the total global river runoff and is sufficient to shut down the THC within 30 years in some models. A freshwater flux of this magnitude is probably not likely for realistic CO_2 scenarios and is more appropriate for glacial meltwater release as proposed for past abrupt

climate change during the Heinrich and Younger Dryas events, but not for 100 years. Figure 9, below, shows the THC intensity results for the models running the 1.0 Sv water-hosing scenario.

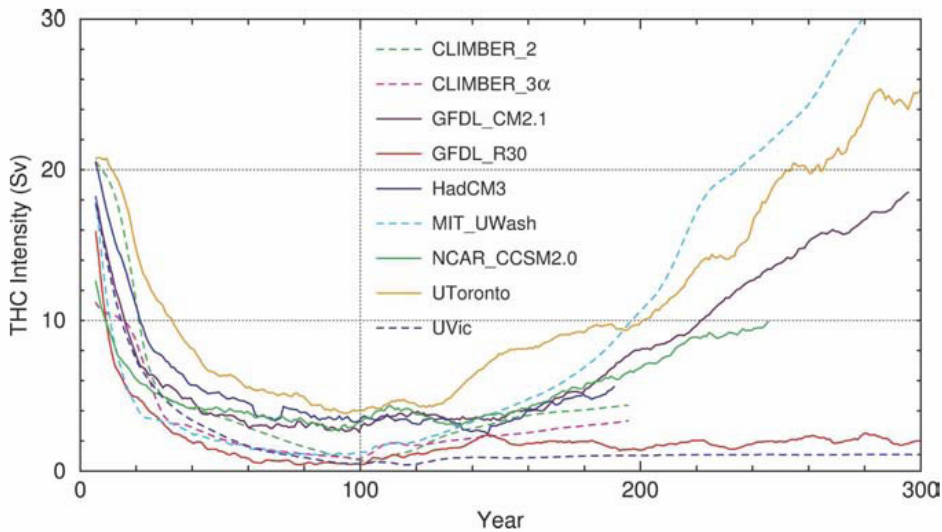


Figure 9: Time Series of THC Intensity (Sv) in 0.1 Sv Water-Hosing Runs
 From (Stouffer et al. 2006): (a) absolute values, (b) relative values to long-term control mean
 AOGCMs: Solid Curves, EMICs: Dashed Curves

In response to 1.0 Sv water-hosing, the THC intensity for all models declines to near shutdown within 50 years. After the termination of freshwater perturbation, some models show rapid re-intensification while others show no trend for recovery.

The following are some of the changes in the model climate (compared to the control runs) due to the freshwater flux and the slowdown of the THC.

- Surface Air Temperature (SAT)
 - Model output varied as to the magnitude of change, but the ensemble mean showed a cooling in the North Atlantic and Western Europe along with a small warming in the Southern Hemisphere.

- Some models showed a significant warming over the Barents and Nordic Seas. It is speculated that this is a response to overturning occurring north of the freshwater perturbation ($> 70^\circ$ N).
- Ocean Temperature and Salinity
 - Sea surface temperatures (SSTs) generally follow the SAT patterns.
 - Sea surface salinity (SSS) patterns are also similar to SST patterns, with freshening in the North Atlantic (due to perturbation) with some models showing increased salinity north of the perturbation ($>70^\circ$ N) around the Barents Sea.
 - There is a SSS increase in the South Atlantic, Caribbean and the Gulf of Mexico, probably due to increased evaporation from warming and shifting precipitation patterns.
- Sea Ice
 - Sea ice in the Labrador Sea increases with a slowdown in the THC
 - Models showing a Barents Sea warming also show a decrease in sea ice in that area
 - At the southern end of the Atlantic (Weddell Sea), there is also a reduction of sea ice with a slowdown of the North Atlantic THC
- Precipitation
 - After the THC slowdown, precipitation increased over the equatorial Atlantic and the Amazon, with a decrease in precipitation over the tropical and sub-tropical Atlantic, including the Caribbean and the Gulf of Mexico

- There is a pronounced southward shift in the Inter Tropical Convergence Zone (ITCZ) and the Hadley circulation (rising equatorial, sinking polar atmospheric circulation), particularly in 1.0 Sv scenario after the THC is shut down. This feature is fairly robust in the AOGCMs but does not appear in the 0.1 Sv EMICs. Figure 10, below, shows the shift in precipitation patterns.

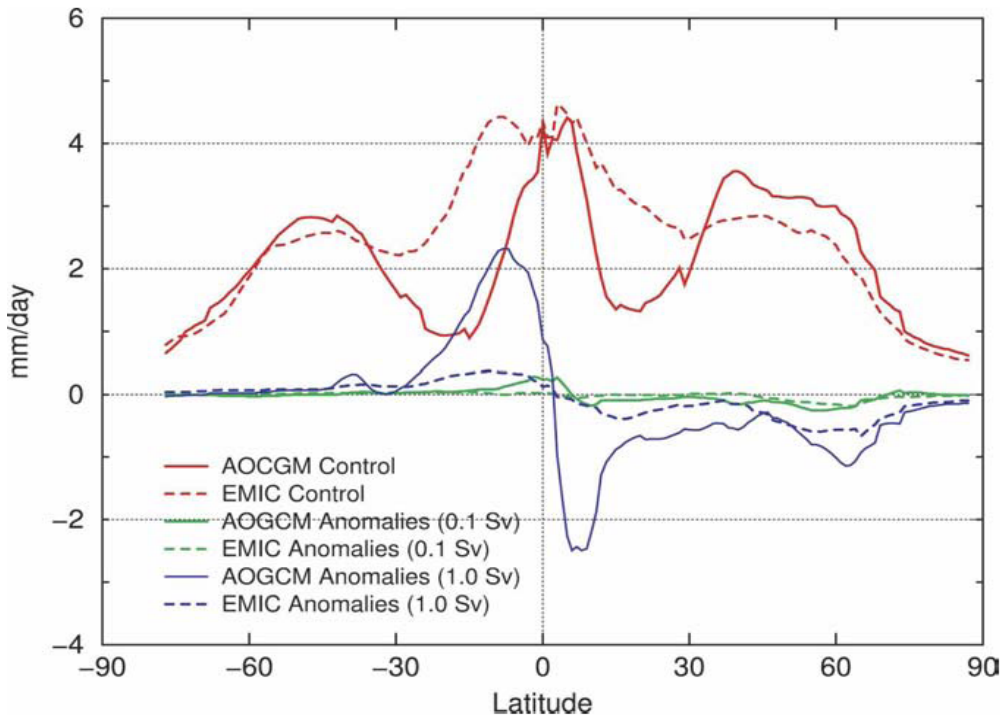


Figure 10: Zonally averaged precipitation over the Atlantic Ocean
 From (Stouffer et al. 2006): Red: control, Green: 0.1 Sv, Blue: 1.0 Sv
Solid line: AOGCM ensemble mean, Dashed line: EMIC ensemble mean

CHAPTER THREE: METHODOLOGY

Research Focus

The focus of this research is to analyze the GFDL 2.1 GCM data output used in (Stouffer et al., 2006) with respects to Tropical Cyclone-Like Vortices (TCLVs) in the North Atlantic basin. TCLV detection was done with a detection scheme applied to the three different freshwater flux (*water-hosing*) scenarios. The identified TCLVs were then analyzed for storm criteria, and then the storms were analyzed for frequency, location and track, with comparisons between the scenarios. Realism or similarity to real-life observational values is addressed with suggestions for future improvements.

Procedures

Data

The Stouffer et al. (Stouffer et al., 2006) study was a [PCMDI](#) (CMIP & PMIP) model intercomparison of EMICs and AOGCMs simulating the response of the THC to fresh water input in the northern North Atlantic. The data used here are from the GFDL CM2.1 AOGCM runs used for that study. The GFDL output is in netCDF file format with a $2^{\circ} \times 2.5^{\circ}$ (latitude \times longitude) grid spacing which represents approximately 140 by 175 statute miles at the equator (~ 69 sm/ $^{\circ}$), and a daily temporal resolution with no leap year (365 days/year).

Approximately 200 GB of data (netCDF) were downloaded from a GFDL ftp site and included global information for the following variables.

- Geopotential height at 1000 hPa, 500 hPa, and 200 hPa

- Precipitation
- Specific humidity at 925 hPa
- Sea level pressure
- Temperature at the surface, 850, 700, 500, and 300 hPa
- Zonal (east-west) and meridional (north-south) wind at 1000 (surface), 200, 300, 850, and 925 hPa
- Vertical wind at 500 hPa

The variables come from the control runs (no hosing), 0.1 Sv hosing runs and the 1.0 Sv hosing runs. Each file included 100 year of output. The control runs included years 101 (start of integration) to 200 and 201 to 300. The 0.1 Sv output from year 101 to 200 included hosing and years 201 to 300 where the hosing was abruptly halted and recovery was simulated. The 1.0Sv output from years 101 to 200 also included hosing with years 201 to 300 and years 301 to 400 for recovery.

Preprocessing

As our interest here is the cumulative effect freshwater flux (water-hosing), the latter part of the hosing period (1st 100 years) output was the target of analysis. This required the reduction, or hyperslaving the year 101 to 200 netCDF files to the last several years of hosing. Using NCO (*ncks* command), the downloaded data were read and new netCDF files were created for the required dates and altitudes (pressure) levels. The downloaded netCDF files themselves had been reduced from the main atmospheric output files to accommodate downloads. The downloads were done using the Linux operating system, since most of the files exceeded the MS Windows

operating system's file capacity of 5GB. The wind and the temperature files contained data for multiple pressure levels and was compressed (packed) as well. To facilitate processing and PC RAM requirements (variables loaded into memory), the files were reduced to yearly (365 day) time slices for a single variable at a single level. The final file sizes, after unpacking, ranged from approximately 2 to 4 GB. Three years (198 – 200) of daily control and water-hosing (0.1 Sv & 1.0 Sv) data for the following variables and levels were used.

- Sea level pressure (variable slp)
- Surface temperature (t_surf)
- Temperatures (temp) at 500 hPa
- Meridional wind (u) at 1000 (~surface) and 850 hPa, in separate files
- Zonal wind (v) at 1000 and 850 hPa, in separate files

The additional variables downloaded, such as precipitation, specific humidity, vertical wind, and geopotential height were not processed at this time as they were not needed for the TCLV detection scheme chosen.

TCLV Detection Script

The detection scheme is written in NCL (NCAR Command Language), and interpretive programming language developed by the National Center for Atmospheric Research (NCAR). Detection was implemented using sea level pressure minima and threshold criteria for vorticity, warm core, and wind velocity. The script is an adaptation of an NCL routine written for the Weather Research Forecast (WRF) Model by Asaha Suzuki, a graduate student in climate research at Georgia Tech.

The general steps used in NCL for data processing are outlined below.

- Libraries used by NCL for data manipulation, processing, and graphics are loaded into memory
- Input data files are opened for reading-in data
- Arrays are allocated for data to be processed as well as storage for the results
- Dimensionally selected (location) data is read and written to arrays
- Data is processed by routines and functions from the loaded libraries
- Results are written to arrays for further processing and output
- Output is via data files, text files, and/or graphics

Daily TCLV detection:

- Area Limits (for the Atlantic basin)
 - Latitude: 50°S:50°N (40°S:40°N effective)
 - Longitude: 0°:100°W (10°W:90°W effective)
- Grid points that are a relative sea level pressure (SLP) minimum to neighboring points are identified with their dates, locations and pressure values written to an array. This location becomes the storm center if all the other criteria are met.
- A 20° × 20° (latitude × longitude) box is defined
- SLP minima points are tested for surface wind threshold criteria and are discarded if they fail
- Remaining points are checked for vorticity criteria and are discarded if they fail
- Remaining points are tested for warm-core criteria and discarded if they fail

- Overlapping ($< 10^\circ$ separation) storm centers are checked for minimum pressure and are discarded if they fail
- Storm centers are written to an array
- TCLV detection repeats for daily increments
- After all days are processed, points that are left are output to data and text files
- Output files are checked for consistency and duration of storms
- Storm centers that are separated by $\sim 10^\circ$ or less on at least two consecutive days are classified as storms

Extraction Parameters

The following detection thresholds, also shown in Table 5 below, were picked for this study.

- Surface wind threshold
 - 10 m/s is picked for this study as being in a middle range for TCLV detection thresholds. The observational threshold for a tropical storm is 17 m/s, but is too high for GCMs since they do not simulate storm intensity realistically due to a coarse resolution. (Camargo & Sobel, 2003) used 10.6 m/s for the Atlantic basin.
- Vorticity threshold
 - 2.5×10^{-5} for vorticity is used for this study and is in the middle range of typically used values. (Camargo & Sobel, 2003) used 2.6×10^{-5} for vorticity in the Atlantic basin.

- Warm core threshold
 - A positive temperature anomaly (> 0) at 500 hPa is used in this study, and was also used in the originally acquired script. (Camargo & Sobel, 2003) used a temperature anomaly of 1.9°C , but it was integrated over three levels. The use of a lower threshold will pick more points that can be filtered later if required.

To achieve realism with observational values, models typically need to be tuned for specific detection parameters. The values picked do not necessarily assume observational realism, but rather results that are reasonable (same order of magnitude) and can be used for comparative statistics.

Table 5
TCLV Detection Threshold Values

<u>Parameter</u>	<u>Threshold Values</u>
Vorticity ($\xi \times 10^{-5}$) at 850 hPa	2.5
Wind Speed (v m/s) at 1000 hPa (~ surface)	10
<u>Temp. Anomaly (δT °C)</u> vorticity (ξ), surface wind (v), and temperature anomaly (δT)	<u>> 0</u>

Post-Processing

The text output produced ~2700 records (~300 /year/scenario for 3 years). The results were manually checked for consistency. Problems with vorticity calculation occurred in approximately 10-15% of the results, where the value returned was “16384” (2^{14}) which passed the threshold criteria, but was not a realistic vorticity value ($\geq 2.5 \times 10^{-5}$). If all the other values were robust (wind, pressure, temp. anomaly), the point was kept to calculate storm duration, but the entire storm was rejected if a realistic vorticity value did not exist for at least 2 consecutive days.

The data were imported into a spreadsheet where storms were determined using the following criteria.

- Points meeting threshold criteria for at least 2 consecutive days where the centers on consecutive days are not separated by more than 10° (lat and/or lon) are considered storms
- Storms centers originating or terminating in the Pacific are considered Atlantic storms if they are located in the Atlantic for at least two consecutive days
- Storms centers inland within 10° of a coastline meeting all other requirements are considered storms
- Storms that could be classified as ‘extra-tropical,’ that is, during winter months and/or at high latitudes ($\sim 40^\circ$ N) are still considered storms if the basic threshold criteria are met

CHAPTER FOUR: FINDINGS

Storm Statistics

It is important to note that GCMs, due to their coarse spatial and temporal resolution, are not able to resolve the dynamics of individual storms (tropical or otherwise). Storm intensity, especially wind speeds are unrealistically low compared to observed values. Storm size is also impossible to define with $2^\circ \times 2.5^\circ$ (~140 by 175 sm) grid spacing and a $20^\circ \times 20^\circ$ (~690 sm from center) detection box. Detection methods can be tuned to a particular GCM to force certain statistics (frequency, etc.) to be comparable to observational values, but storm characteristics influenced by microscale dynamics do not simulate realistically because of a coarse resolution.

It is also important to note that these results are for only three years and that a greater sample would provide more reliable results. As this study is ongoing, more records are being added. On the other hand, I suspect that the model output may not have the range of variability found in nature. Examination of individual yearly records reinforces some of the trends observed in the averages.

Frequency

Overall storm frequency seems to decrease as water-hosing is applied as shown in Figures 11 & 12, and Table 6 below. The monthly averages are inconclusive for the small sample size and are biased towards a higher value because if a storm overlaps months, it is counted once for each month. The average annual decrease is significant, especially between the control and 1.0 Sv scenario, where the decrease is 22.1% (Table 6).

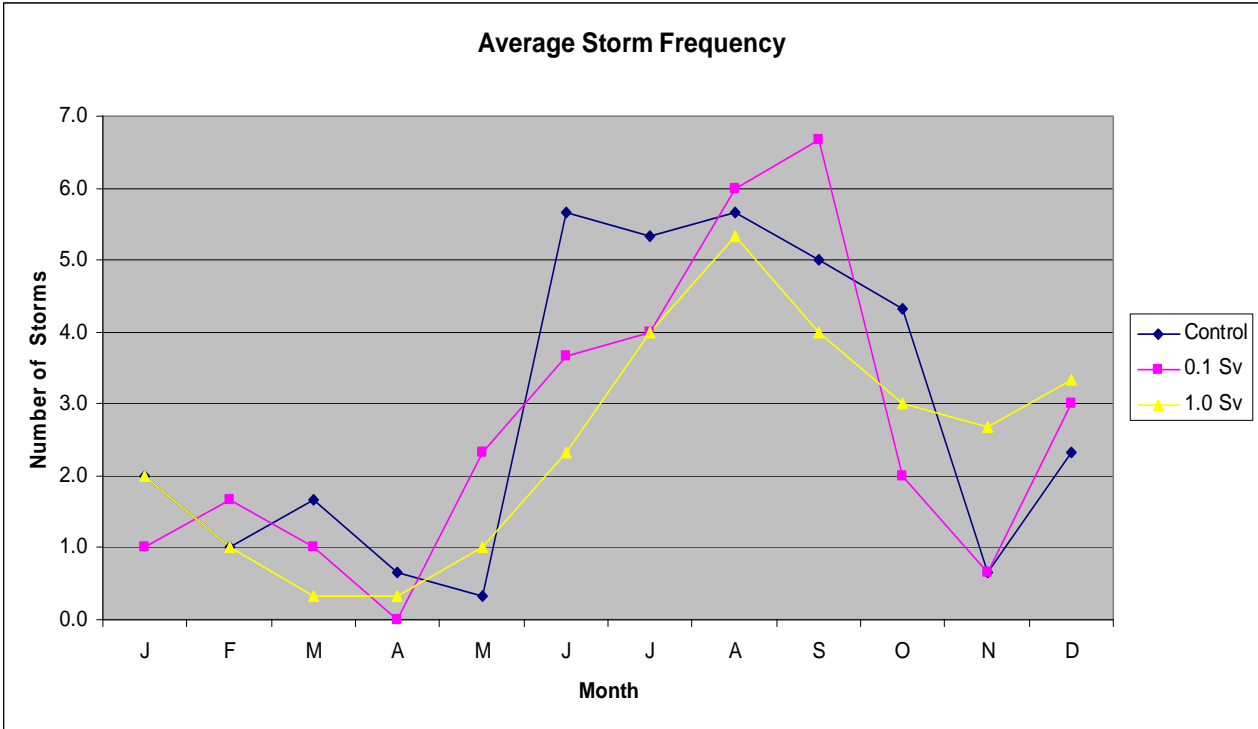


Figure 11: Average Monthly Storm Frequency

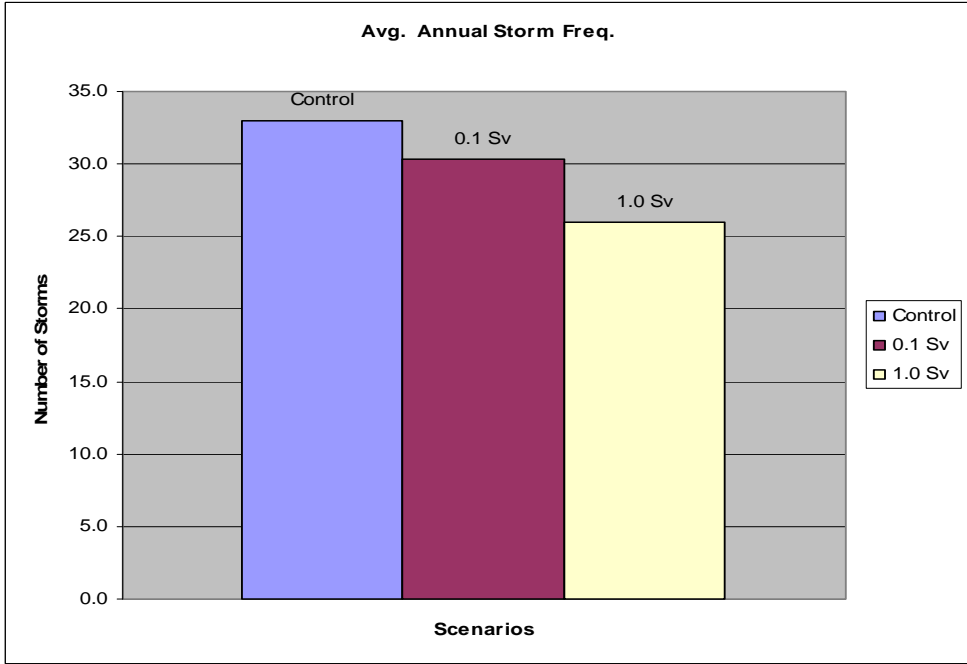


Figure 12: Average Annual Storm Frequency

Table 6
Average Storm Frequencies

<u>Scenario</u>	<u>Average Storm Frequency</u>	
	<u>Tot</u>	<u>%Change</u>
Control	33.0	
0.1 Sv	30.3	-8.1
<u>1.0 Sv</u>	<u>26.0</u>	<u>-21.2</u>

Storm Days

The average amount of storm days also decreases with an increase in water-hosing. The monthly averages still suffer from a small sample size, but trend towards a later start in the tropical season with more late-season storms, especially in the 1.0 Sv scenario, as shown in Figure 13. The annual averages of the three scenarios show an inverse relationship between hosing and the number of average annual storms, with a reduction 7.3% and 16.3% for the 0.1 Sv and 1.0 Sv scenarios, respectively (Table 7 and Figures 12 & 13).

Table 7
Average Annual Storm Days

<u>Scenario</u>	<u>Average Annual Storm Days</u>	
	<u>Tot</u>	<u>%Change</u>
Control	114.3	
0.1 Sv	106.0	-7.3
<u>1.0 Sv</u>	<u>95.7</u>	<u>-16.3</u>

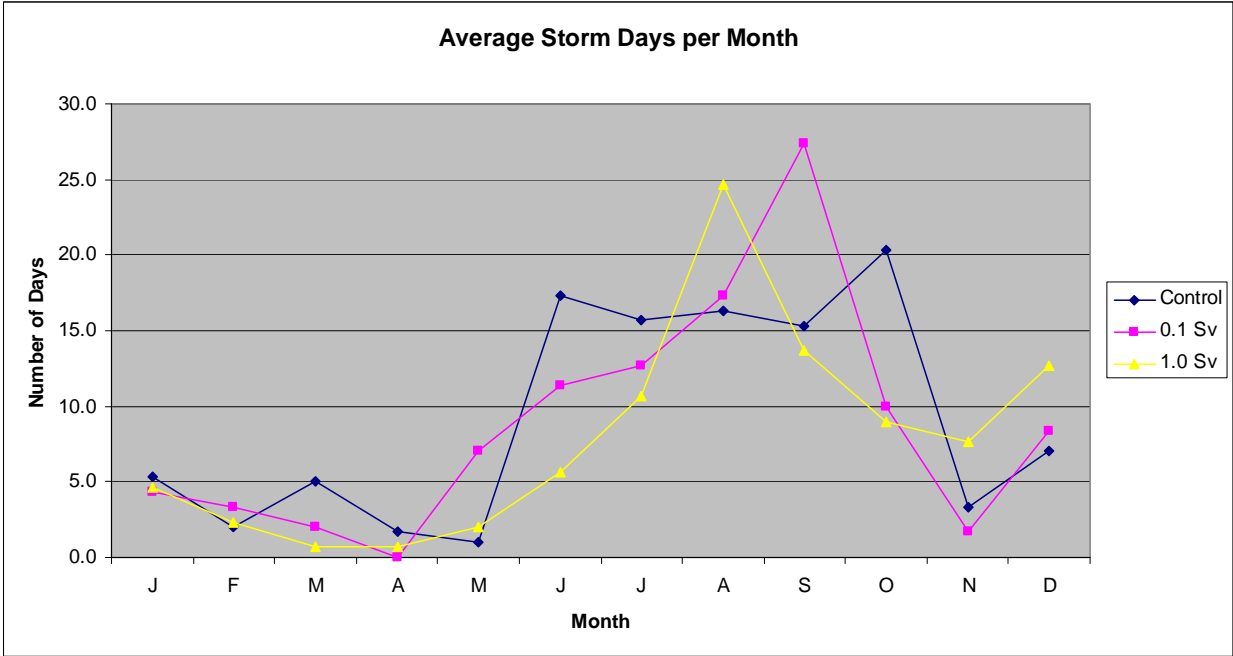


Figure 13: Average Monthly Storm Days

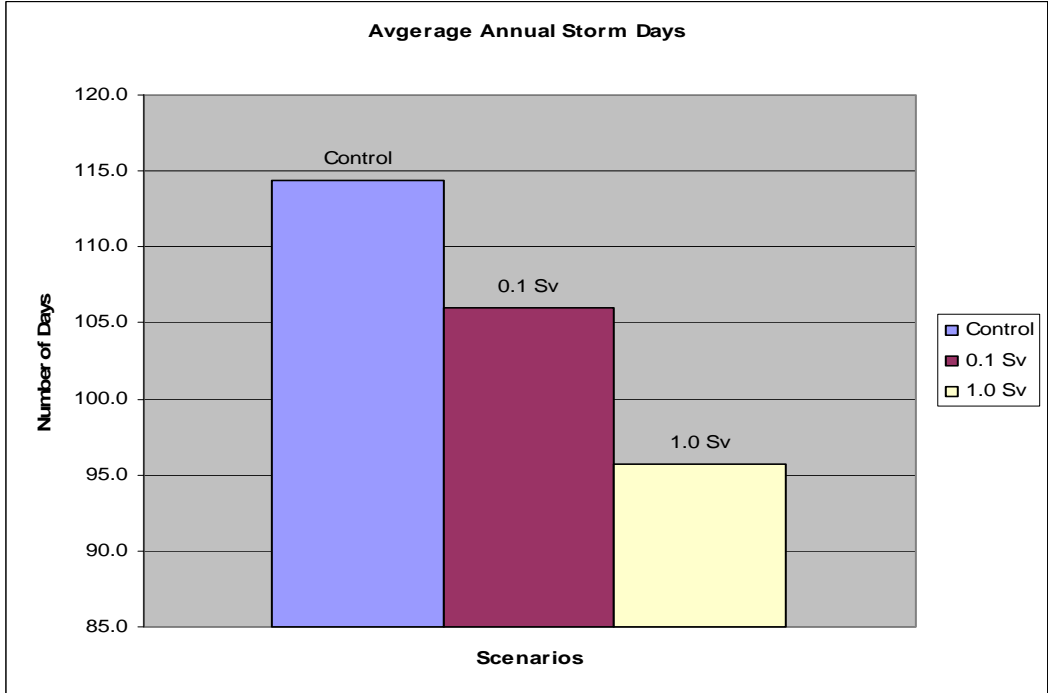


Figure 14: Average Annual Storm Days

Duration

Statistics for storm duration are for average storm duration (storms/storm days) and the average of the longest storms for each year for each scenario. Table 8 summarizes the duration statistics, with plots in Figures 15 & 16 for monthly and annual averages, and Figures 17 & 18 for maximum monthly and annual averages.

From the results, the average storm duration increases directly with the amount water-hosing. The average storm duration increases by 2.7% and 7.4% compared to the control scenario, while the average of maximum length storms increases by 33.3% and 48.1% for 0.1 Sv and 1.0 Sv scenarios, respectively.

Trends from the storm frequency and duration statistics seem to indicate that as the amount of water-hosing increase, the number of storms decrease, as well as the total storm days, but the storms get longer.

While still suffering from inadequate sample size (noise, etc.), the monthly plots all seem to show a temporal shift to a later storm season for the 1.0 Sv scenario

Table 8
Average Annual Storm Duration

Scenario	<u>Average Annual Storm Duration</u>			
	Avg (days)	% Change	Max (days)	% Change
Control	3.4		9.0	
0.1 Sv	3.5	2.7	12.0	33.3
1.0 Sv	3.7	7.4	13.3	48.1

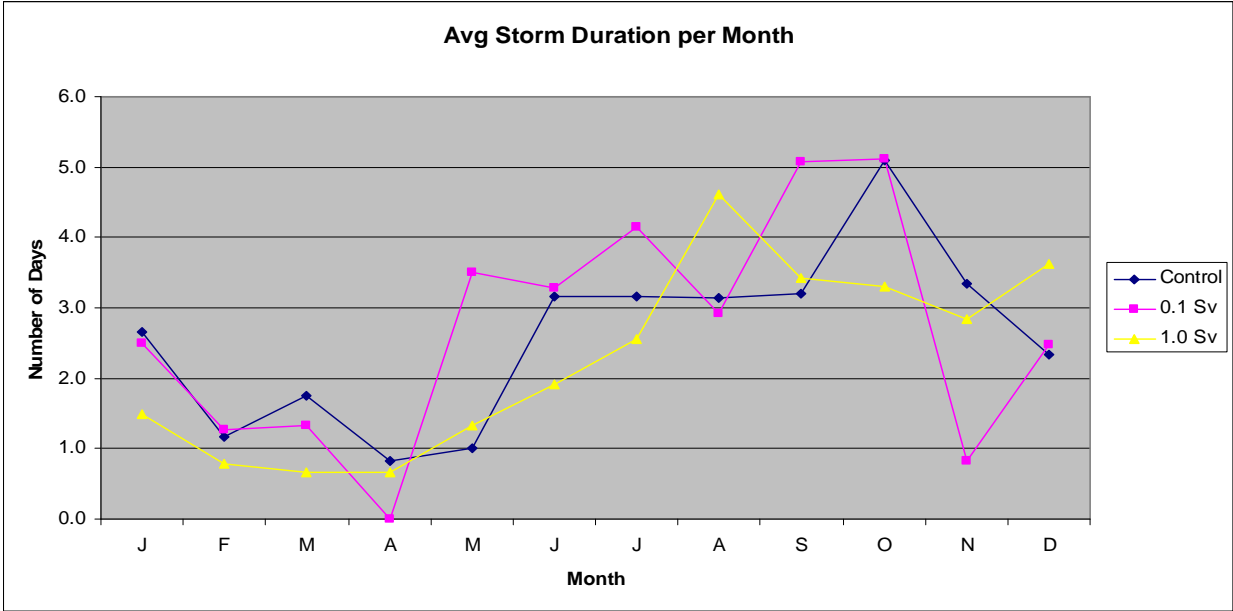


Figure 15: Average Monthly Storm Durations

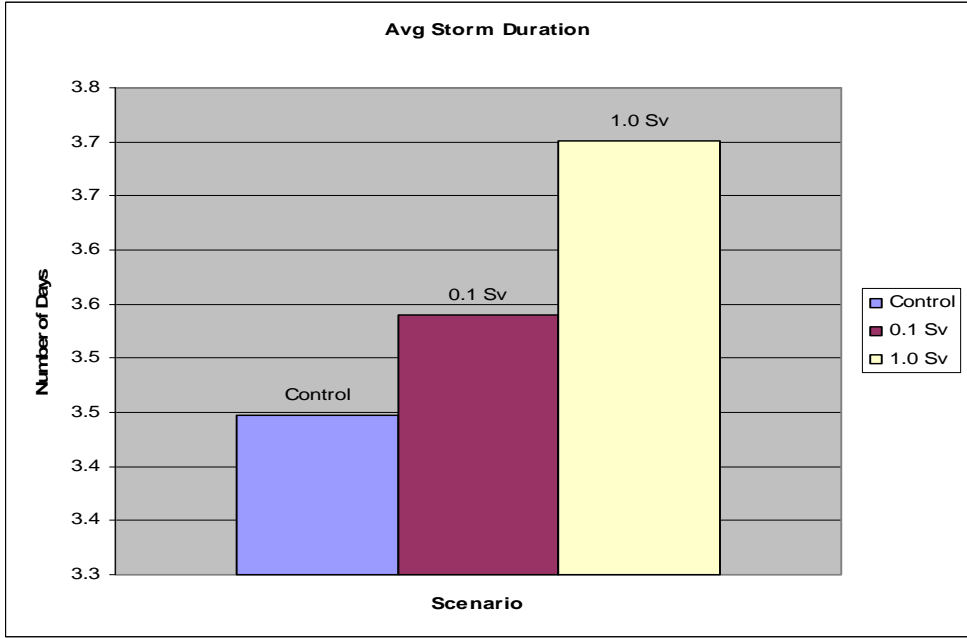


Figure 16: Average Annual Storm Duration

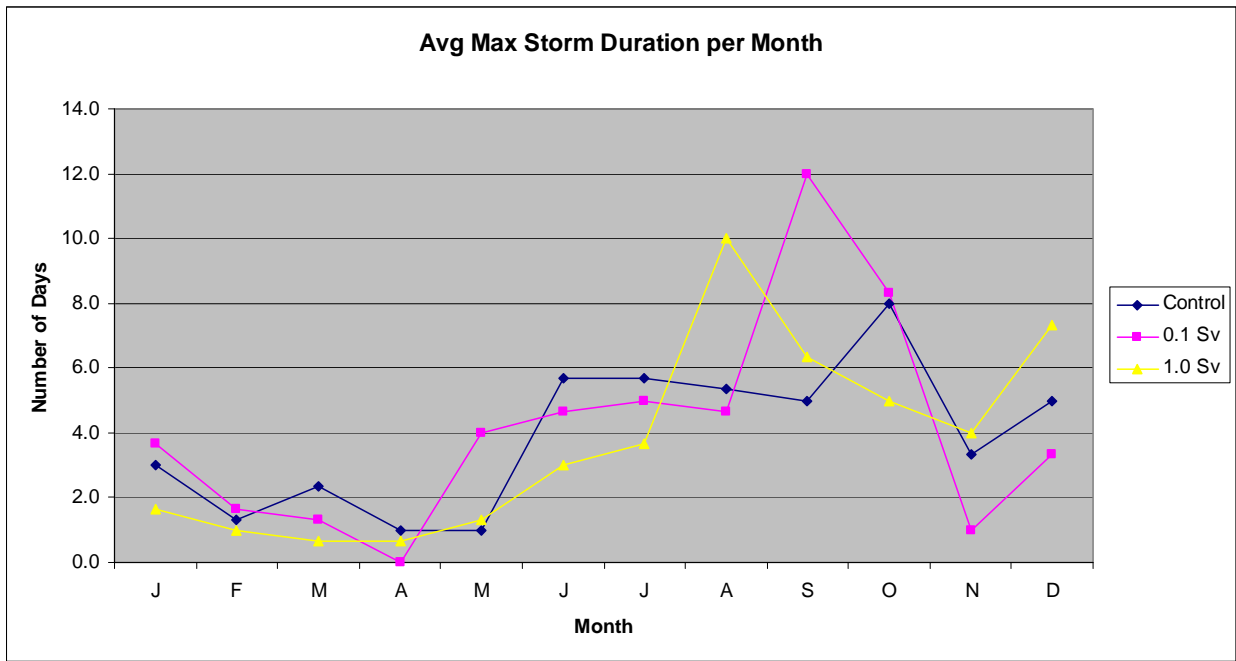


Figure 17: Average Maximum Monthly Storm Durations

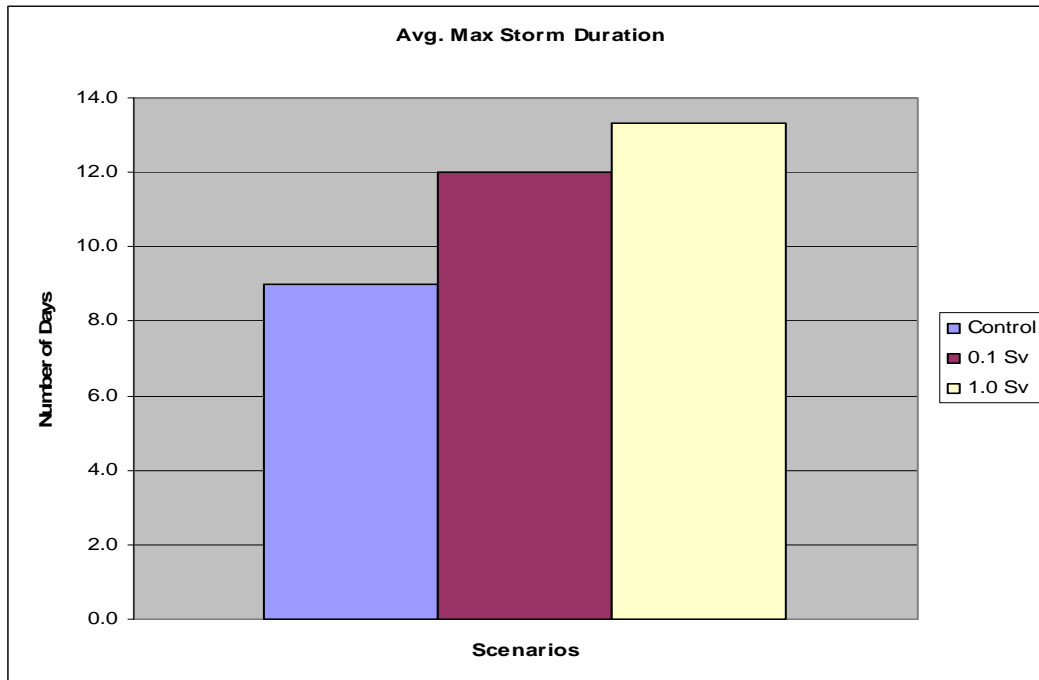


Figure 18: Average Annual Maximum Storm Durations

Location

Location will be looked at from the perspective of coordinates (latitudes and longitudes) as well as geographic areas.

Latitude & Longitude

Averages and modes for storm latitudes and longitudes are shown in Table 9. The averages do not show much differentiation in latitude and an approximate 5° westward shift for the 0.1 Sv scenarios. The latitude modes show a direct shift southward for water-hosing scenarios, regardless of amount. The longitude modes show a significant shift westward for 0.1 Sv and a smaller shift westward for the 1.0 Sv scenarios. The latitude distributions in Figures 19 & 20 (sorted) show the significant southward shift in the hosing scenarios. The longitude distributions in Figures 21 & 22 (sorted), show the westward in the hosing scenarios, with the 1.0 Sv simulation balancing the westward shift with an increase coastal African (< 30° W) and South American (~60° W) activity.

Table 9
Average Latitudes & Longitudes

Scenario	<u>Latitudes & Longitudes – Averages & Modes</u>			
	Lat N (Avg	Mode)	Lon W (Avg	Mode)
Control	18.08	23.26	62.46	51.25
0.1 Sv	18.04	19.21	67.38	86.25
1.0 Sv	18.31	19.21	62.22	56.25

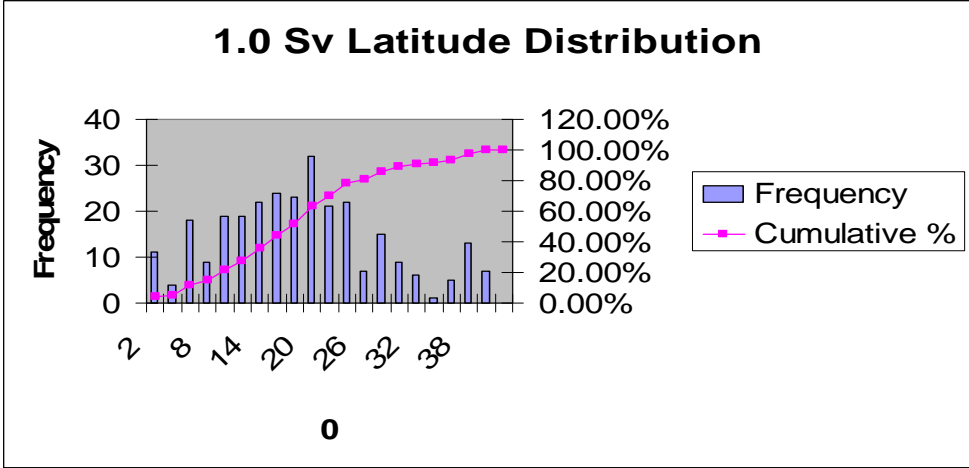
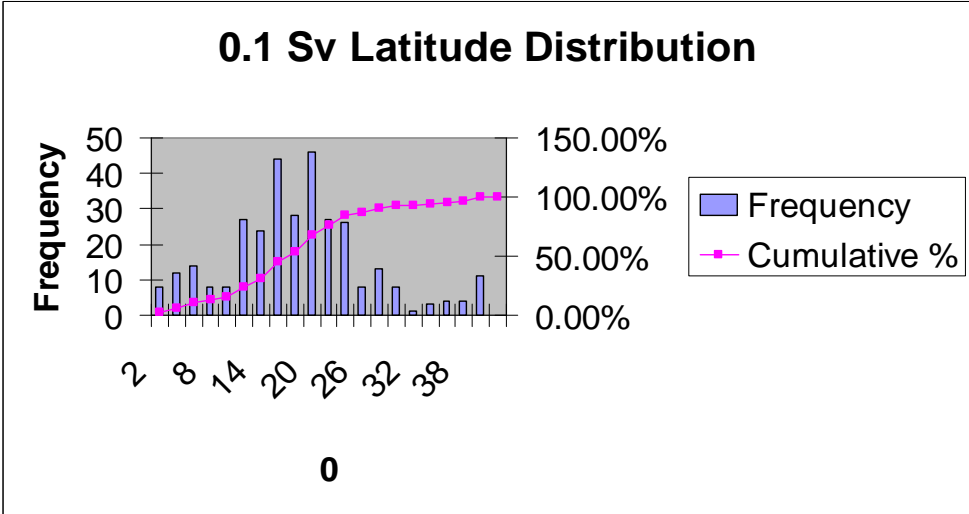
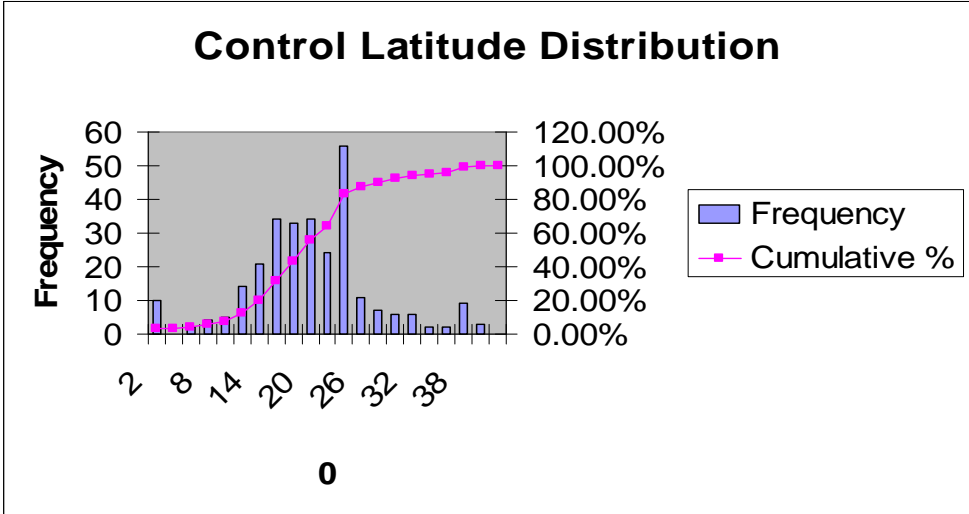


Figure 19: Latitude Distributions

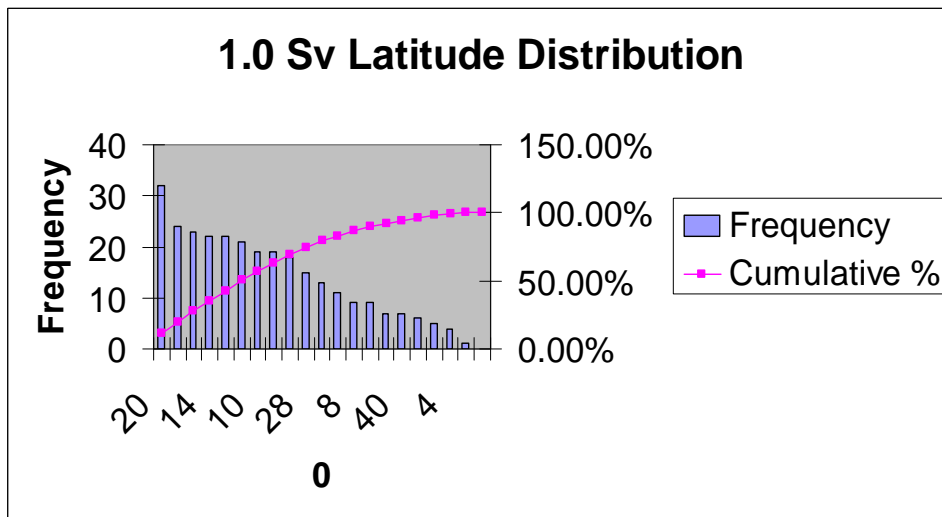
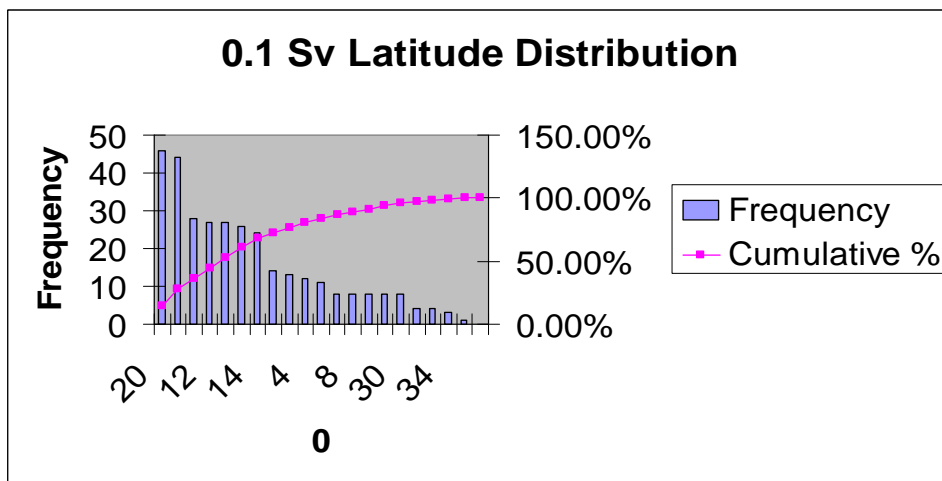
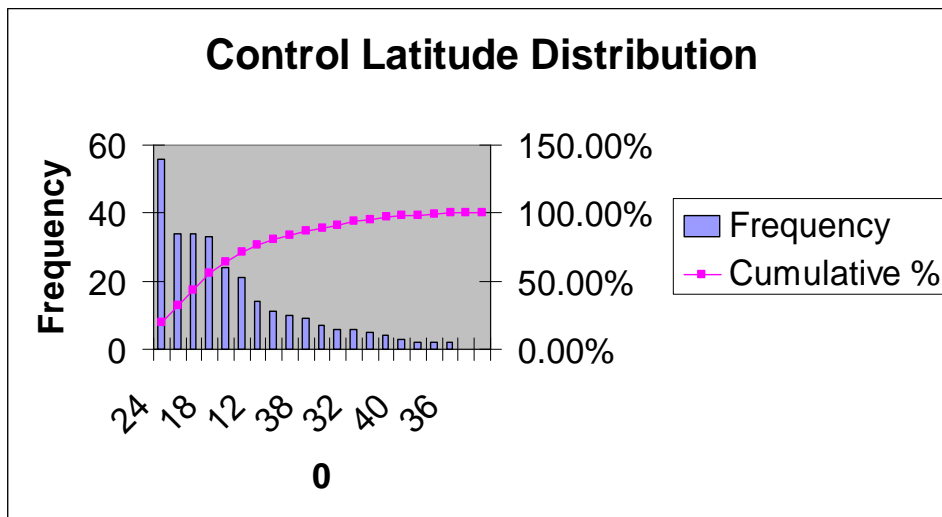


Figure 20: Sorted Latitude Distributions

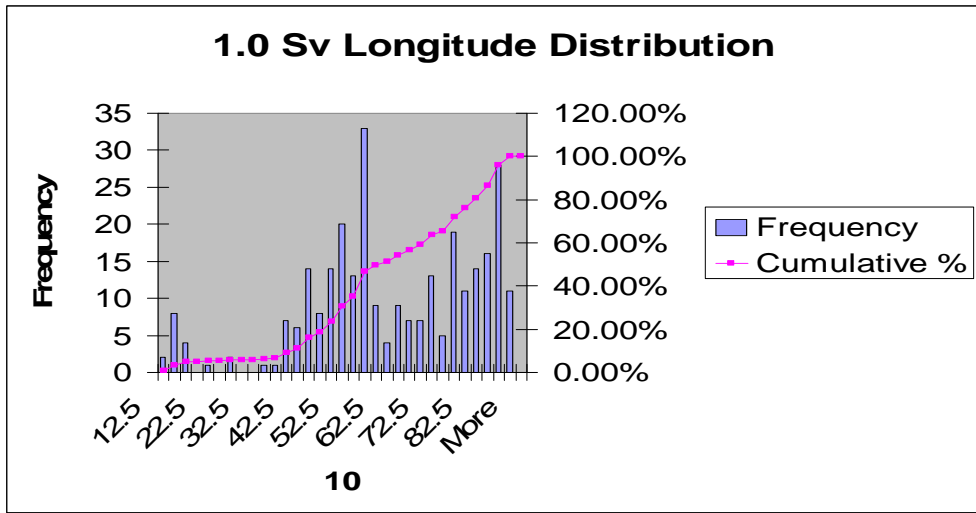
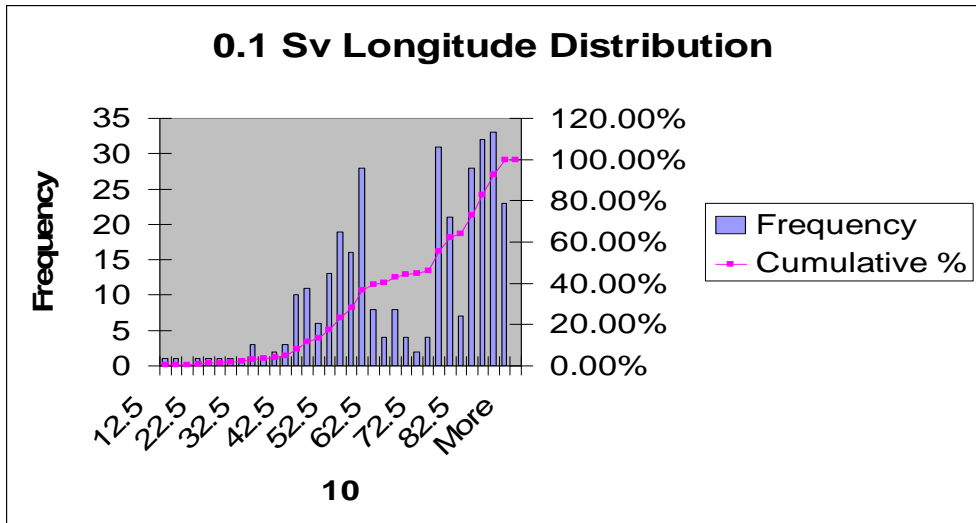
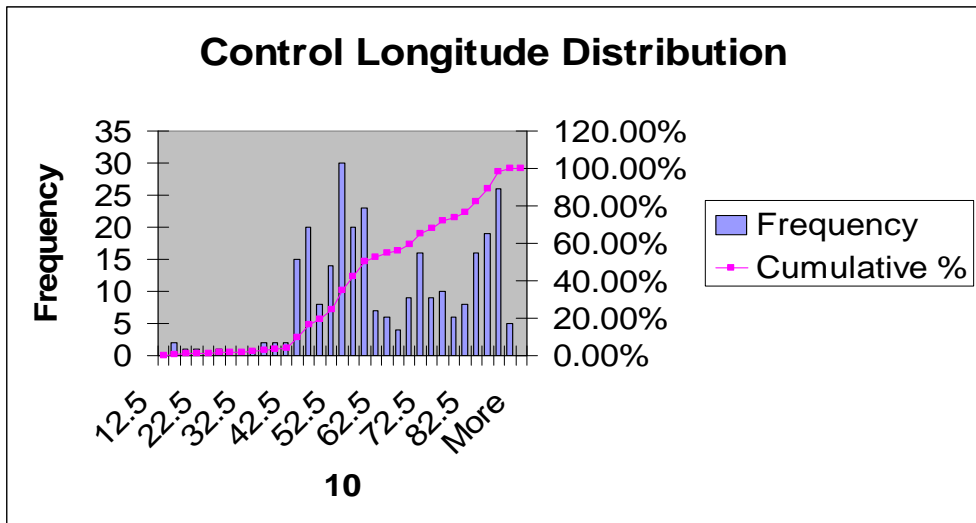
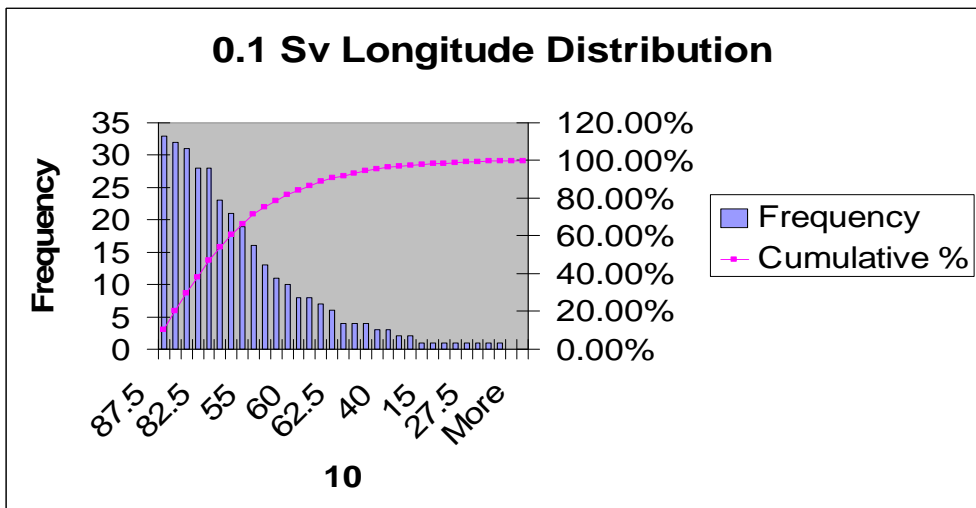
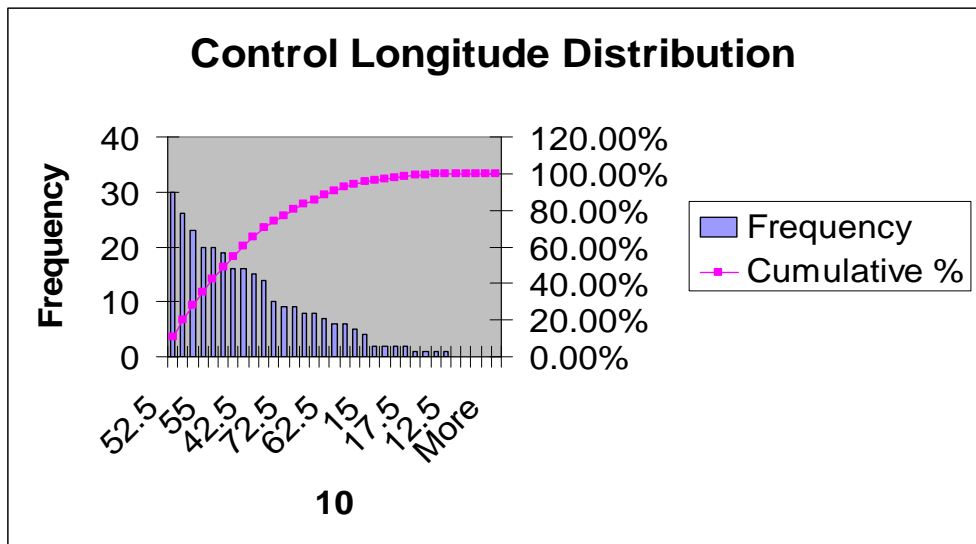


Figure 21: Longitude Distributions



Geographic Area

To try to get a feel for the area distribution and changes, the following were subjectively chosen.

- 1 - Open Ocean (OE): $< 10^{\circ}$ N (equatorial)
- 2 - Open Ocean (OE): 10° - 30° N
- 3 - Open Ocean (OE): $> 30^{\circ}$ N
- 4 - Caribbean East (in the area of the Lesser Antilles)
- 5 - Caribbean Central (~between Hispaniola and South American coast)
- 6 - Caribbean West (~between Central America and Cuba)
- 7 - Bahamas - Florida Straits – North Cuba
- 8 - Gulf of Mexico
- 9 - US East Coast
- 10 - African Coast - North
- 11 - African Coast - Equatorial
- 12 - South American Coast – N to NE

The first set of frequency distributions (Figure 23) can be a little misleading since the average number of storms decreased with increase in water-hosing. The second sets of distributions (Figure 24) are percentage frequencies, so are more comparable. The 0.1 Sv scenario shows a slight decrease on open ocean (1, 2, & 3) activity, a decrease in the eastern Caribbean (4), a significant increase in the central & western Caribbean, and Florida-Bahamas (5, 6, & 7), and increases off the eastern US and South American coasts. The 1.0 Sv scenario also has decreased open ocean activity, a significant decrease in all Caribbean and Florida-Bahamas areas, the only storm in the Gulf of Mexico, and a significant increases in activity off the African coast (to all scenarios), and an increase off the South American coast (compared to control). Figure 25 summarizes the area percentage distribution changes in a single chart.

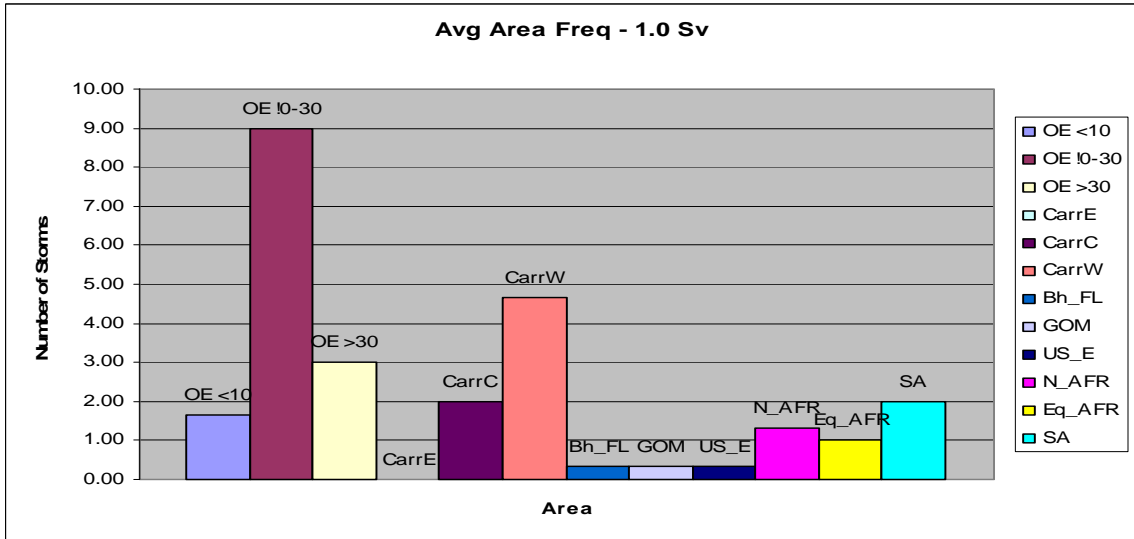
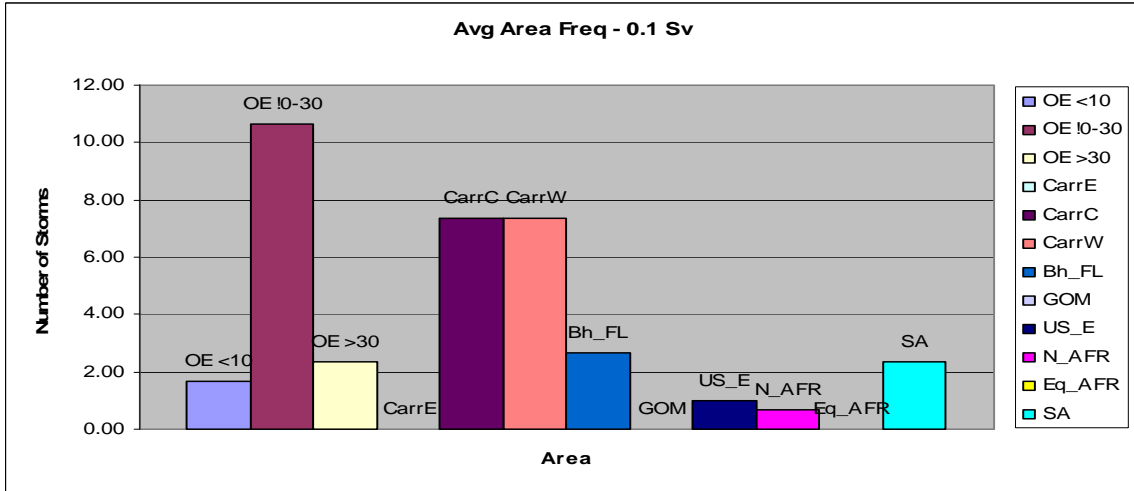
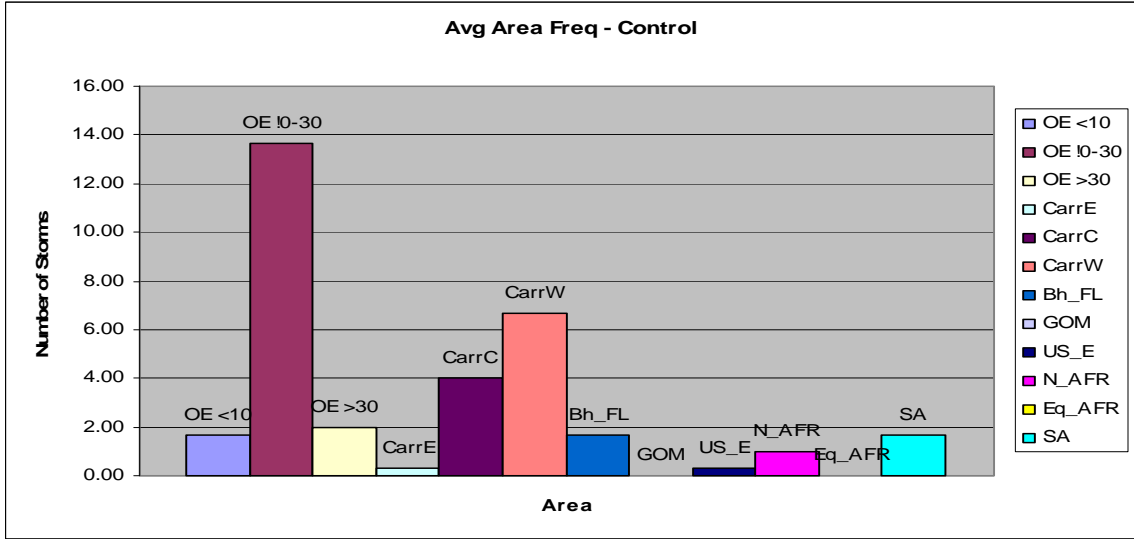


Figure 23: Average Area Frequency Distribution

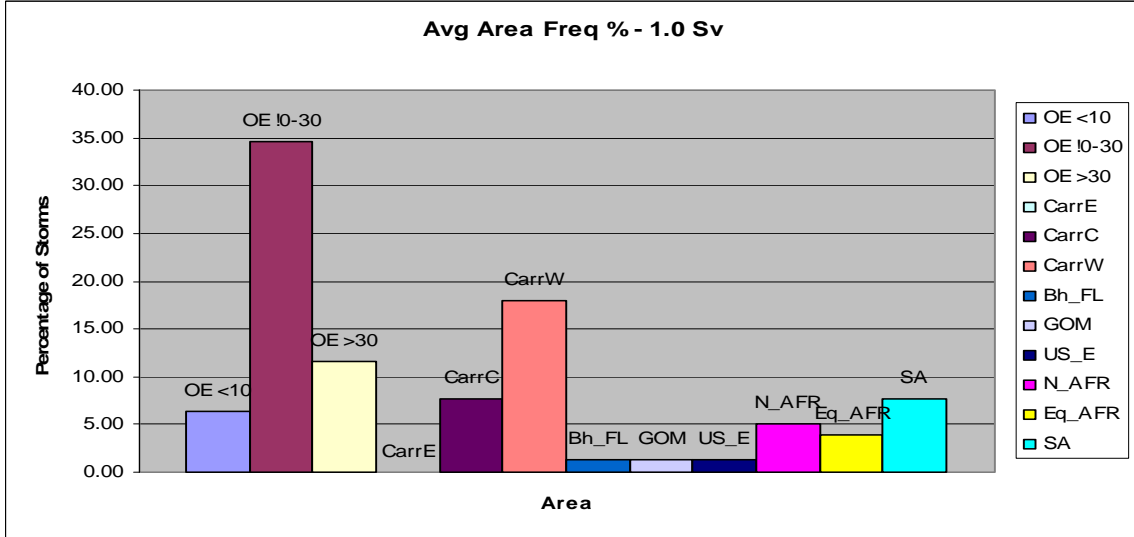
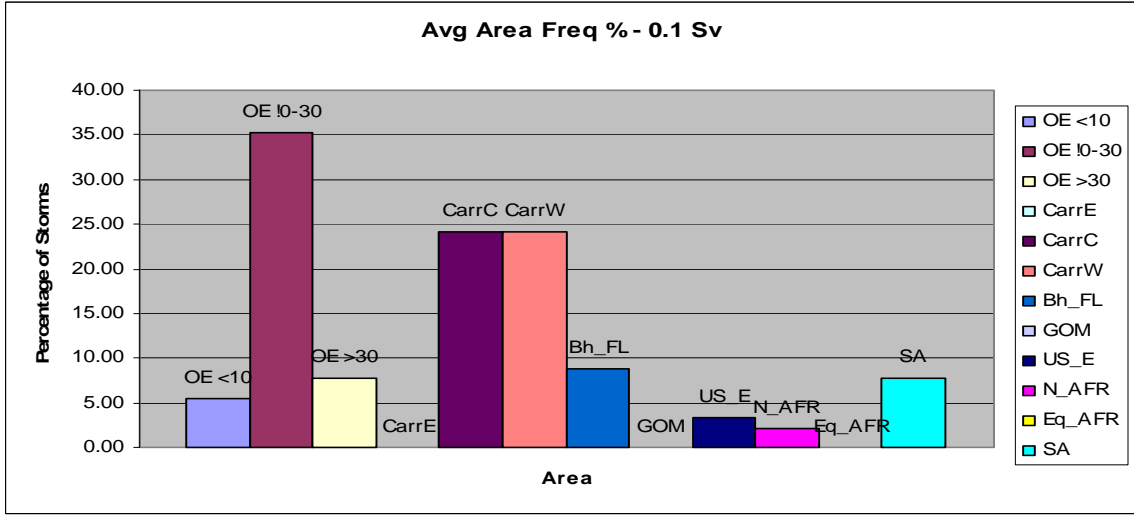
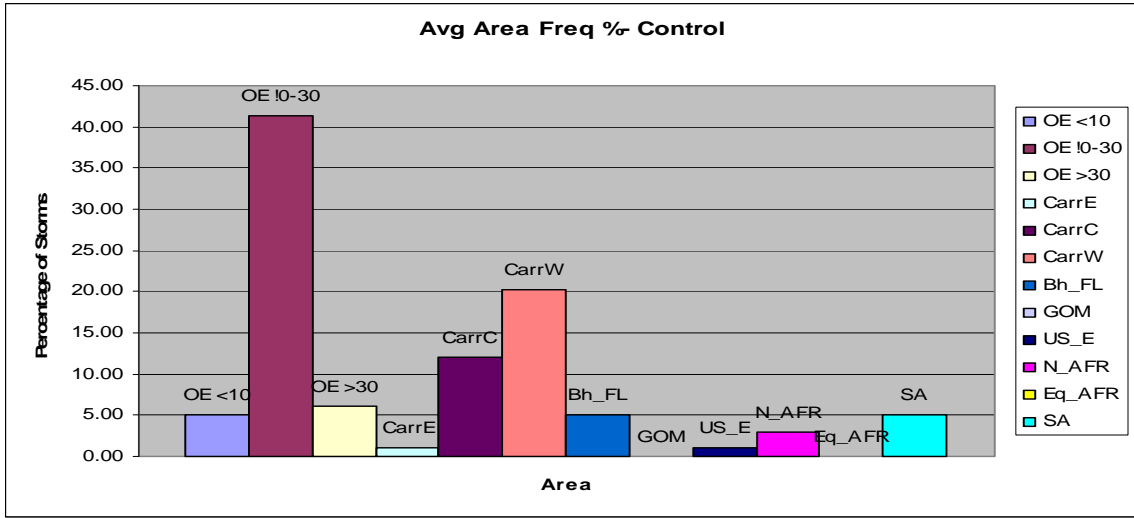


Figure 24: Average Area Percentage Distribution

westbound or eastbound is not realistic. I suspect that the inability of the GFDL CM2.1, with a resolution of $2^\circ \times 2.5^\circ$ (latitude \times longitude), to resolve the microscale storm dynamics and interactions, contributes to the failure to realistically simulate the mechanisms that propel storm in a particular direction.

Table 10
Average Zonal Storm Track Percentage

Scenario	<u>Average Zonal Track Percentage</u>		
	<u>% Westbound</u>	<u>% Stationary</u>	<u>% Eastbound</u>
Control	26.7	44.4	29.3
0.1 Sv	34.1	42.9	23.1
1.0 Sv	24.7	50.0	26.6

Pressure, Wind, Vorticity & Temperature Anomaly

Table 11, below, list the maximum and mean values for pressure, wind, vorticity, and temperature anomaly obtained during this project. These values, while representative of the storms detected in this study, do not offer much information other than the limitations of the small sample size and the inability of the GFDL CM2.1 GCM to resolve storm dynamics realistically. While the pressure values are reasonable, lower observational values have been recorded (Wilma (2005) – 882 mb, Gilbert (1988) – 888.2 mb, etc.) suggesting that there are not enough samples, a limited dynamic range, or both. That the maximum wind values barely qualify for tropical storm status (≥ 17 m/s), let alone tropical cyclone status (≥ 33 m/s) underscores the GCM’s inability to realistically simulate tropical cyclone intensity.

Table 11
 Pressure, Wind, Vorticity, and Temperature Anomaly Values

Scenario	Pressure (mb)		Wind (m/s)		Vorticity ($\times 10^{-5}$)		Temp. Anom.	
	Min	Mean	Max	Mean	Max	Mean	Max	Mean
Control	987.07	999.51	18.07	13.07	7.49	3.51	4.44	0.76
0.1 Sv	988.69	1001.59	18.86	12.84	7.20	3.44	4.30	0.71
1.0 Sv	979.74	1000.99	17.66	12.75	8.08	3.61	5.25	0.94

CHAPTER FIVE: CONCLUSION AND SUMMARY

Statistical Conclusions

Conclusions drawn from the results presented in the previous chapter on the analysis of simulated tropical storms derived from tropical cyclone-like vortices (TCLVs) in the GFDL CM2.1 model output used in the Stouffer (Stouffer et al., 2006) freshwater perturbation study are summarized here.

As detailed previously, three simulation scenarios were run. The control run was based on 1860, pre global warming conditions, with no freshwater flux perturbation (water-hosing). The other two runs had increasing amounts water-hosing, 0.1 Sv and 1.0 Sv, applied uniformly between 50° and 70°N latitude in the North Atlantic. Details are found earlier in this document.

The following statistics and observations were concluded and are summarized in Table 12, below.

- As water-hosing increased
 - Average number of annual storms decreased
 - Average number of storm days decreased
 - Average and maximum durations of storms increased
 - Distribution of storms shifted southward and westward (and eastward for 1.0 Sv)
- 0.1 Sv scenario
 - 8.1% fewer storms
 - 7.3% fewer storm days
 - Average storm duration increased 2.7%

- Maximum storm duration increased 33.3%
- Latitude (mode) shifts ~ 4° to the south (to 19.21°N)
- Longitude (mode) shifts ~ 35° to the west (to 86.25°W)
- 1.0 Sv scenario
 - 21.2% fewer storms
 - 16.3% fewer storm days
 - Average storm duration increased 7.4%
 - Maximum storm duration increased 48.1%
 - Latitude (mode) shifts ~ 4° to the south (to 19.21°N)
 - Longitude (mode) shifts ~ 6° to the west (to 56.25°W)
 - Westerly shift, but balanced by increased activity of the African coast (< 30°W)
- For all scenarios
 - Storm track and intensities are unrealistic in this model output
 - Only 1 storm in the Gulf of Mexico (unrealistic), none south of the equator

Table 12
Summary of Average Statistics and Changes for 0.1 Sv & 1.0 Sv (vs. Control)

Scenario	<u>Statistics</u>					
	Strms	Days	Duration (Avg)	Max)	Lat°N(Mode)	Lon°W(Mode)
Control	33.0	114.3	3.4	9.0	23.26	51.25
0.1 Sv	30.0(-8.1%)	106.0 (-7.3%)	3.5 (2.7%)	12.0(33.3%)	19.21(-4)	86.25(+35)
1.0 Sv	26.0(-21.2%)	95.7 (-16.3%)	3.7 (7.4%)	13.3(48.1%)	19.21(-4)	56.25(+5)

The results above correlate with the climate changes observed in (Stouffer et al., 2006), especially the southerly displacement of the Inter-Tropical Convergence Zones (ITCZ) and precipitation patterns shown in Figure 10. The ITCZ shift correlates to the southerly shift in storm distribution. The southerly shift of precipitation pattern, especially for the 1.0 Sv scenario where precipitation shifts to the equatorial Atlantic with a decrease in the tropical Atlantic and Caribbean, correlates with the decrease of storms overall and especially in those areas.

Relevance of Results

As stated earlier, GCMs, especially those with coarse-to-medium resolutions as used in this study, are not very suitable to simulate tropical cyclones in detail, but are excellent models, to study long-term and slowly varying phenomena like ocean currents. Nevertheless, I believe that tropical cyclone detection in GCMs can provide very useful information, especially about those parameters that influence cyclone genesis.

Continuation and Suggestions

More ideal models to simulate the influence of ocean current changes on tropical weather would be the higher-resolution regional models with nesting (downscaling) parameterized with GCM-obtained values, higher resolution GCMs, or a combination of GCMs with high-resolution nested regional models through a common framework/interface such as ESMF facilitated by advances in both modeling and computational technology. My future plans include running idealized tropical storm simulations in the Weather Research & Forecast (WRF)

model parameterized by GCM data (including data used in this study) as well as participating in ESMF development.

The work presented here is ongoing, as I am in the process of adding additional years of data as well as making modifications in the TCLV detection routine to hopefully produce and publish more comprehensive results.

LIST OF REFERENCES

- Broccoli, A. J., & Manabe, S. (1990). Can existing climate models be used to study anthropogenic changes in tropical cyclone climate? *Geophysical Research Letters*, 17(11), 1917-1920.
- Bryden, H., Longworth, H. R., & Cunningham, S. A. (2005, 1 December). Slowing of the Atlantic meridional overturning current at 25 degrees N. *Nature*, 138.
- Camargo, S. J., & Sobel, A. H. (2003, 4 December). Formation of tropical storms in an atmospheric general circulation model. *Tellus*, 56(A), 56-67.
- Camargo, S. J., & Zebiak, S. E. (2002). *Improving the detection and tracking of Tropical Cyclones in Atmospheric General circulation Models* (The International Research Institute For Climate Prediction No. 02-02). Columbia University in the City of New York: Columbia Earth Institute.
- Center for Global Environment. (2004, 21 October). *Hurricanes and Global Warming News Conference* (Stapf, S. E., Ed.). .
- Emanuel, K. (2005, 4 August). Increasing destructiveness of tropical cyclones over the past 30 years. *Nature*, 436, 686-688.
- Final Report of the Technical Workshop on WRF-ESMF Convergence*. Author. (2006). Boulder, CO.
- Goldenberg, S. B., Landsea, C. W., Mesta-Nunez, A. M., & Gray, W. M. (2001, 20 July). The recent increase in Atlantic hurricane activity: Causes and implications. *Science*, 293, 474-479.

- Gray, W. M. (1968, October). Global View Of The Origin Of Tropical Disturbances And Storms. *Monthly Weather Review*, 96(10), 669-700.
- Gray, W. M. (1979). Hurricanes: Their formation, structure, and likely role in tropical circulation. In D. B. Shaw (Ed.), *Meteorology over Tropical Oceans* (pp. 155-218). Royal Meteorological Society.
- Gray, W. M. (1984, September). Atlantic seasonal hurricane frequency. Part 1: El Nino and 30 mb quasi-biennial oscillation influences. *Monthly Weather Review*, 112, 1649-1668.
- Gray, W. M., & Klotzbach, P. J. (2005, 2 September). Forecast of Atlantic hurricane activity for September and October 2005 and seasonal update through August. Retrieved 5 May 2006, from Department of Atmospheric Science: <http://hurricane.atmos.colostate.edu/forecasts/2005/sep2005/>.
- Hakkinen, S., & Rhines, P. B. (2004, 23 April). Decline of subpolar North Atlantic circulation during the 1990s. *Science*, 305, 555-559.
- Hansen, J. (2006, 17 February). Climate Change: On the Edge. *The Independent (UK)*.
- Intergovernmental Panel on Climate Change (Working Group I). (2007a). *Summary for Policymakers, IPCC WGI Fourth Assessment Report*. (Vol. Climate Change 2007: The Physical Science Basis). Geneva, Switzerland: IPCC Secretariat c/o WMO.
- Intergovernmental Panel on Climate Change (Working Group II). (2007b). *Summary for Policymakers, IPCC WGII Fourth Assessment Report*. (Vol. Climate Change 2007: Climate Change Impacts, Adaptation and Vulnerability). Geneva, Switzerland: IPCC Secretariat c/o WMO.

- Intergovernmental Panel on Climate Change (Working Group III). (2007c). *Summary for Policymakers, IPCC WGIII Fourth Assessment Report*. (Vol. Climate Change 2007: Mitigation of Climate Change). Geneva, Switzerland: IPCC Secretariat c/o WMO.
- Kerr, R. A. (2007, 1 June). Mammoth-Killer Impact Gets Mixed Reception From Earth Scientists. *Science*, 316(5829), 1264-1265.
- Klotzbach, P. J. (2006, 2 March (revised)). Trends in Global Tropical Cyclone Activity over the Past Twenty Years (1986-2005). *Geophysical Research Letters*, submitted 27 January 2006.
- Knutson, T. R., & Tuleya, R. E. (1999). Increased hurricane intensities with CO₂-induced warming as simulated using the GFDL hurricane prediction system. *Climate Dynamics*, 15, 503-519.
- Knutson, T. R., & Tuleya, R. E. (2004, 15 September). Impact of CO₂-induced warming on simulated hurricane intensity and precipitation: Sensitivity to the choice of climate model and convective parameterization. *Journal of Climate*, 17(18), 3477-3495.
- McGuffie, K., & Henderson-Sellers, A. (2005). *A Climate Modelling Primer, Third Edition*. West Sussex, England: John Wiley & Sons, Ltd.
- Nguyen, K. C., & Walsh, K. J. E. (2001, 1 July 2001). Interannual, Decadal, and Transient Greenhouse Simulation of Tropical Cyclone-like Vortices in a Regional Climate Model of the South Pacific. *Journal of Climate*, 14, 3043-3054.
- Ottera, O. H., Drange, H., Bentsen, M., Kvamsto, N. G., & Jiang, D. (2004, 29 January). Transient response of the Atlantic Meridional Overturning Circulation to enhanced freshwater input to the Nordic Seas - Arctic Ocean in the Bergen Climate Model. *Tellus*, 56A, 342-361.

- Petit, J. R., Jouzel, J., Raynaud, D., Barkov, N. I., Barnola, J.-M., Basile, I. et al. (1999, 3 June). Climate and atmospheric history of the past 420,000 years from the Vostok ice core, Antarctica. *Nature*, 399, 429-436.
- Pielke, R. A. J., Landsea, C., Mayfield, M., Laver, J., & Pasch, R. (2005, November). Hurricanes and Global Warming. *American Meteorological Society*, pp. 1571-1575.
- Rahmstorf, S. (2002, 12 September). Ocean circulation and climate during the past 120,000 years. *Nature*, 419, 207-214.
- Siegenthaler, U., Stocker, T., Monnin, E., Luhti, D., Schwander, J., Stauffer, B. et al. (2005, 25 November). Stable Carbon Cycle-Climate Relationship During the Late Pleistocene. *Science*, 310, 1313-1317.
- Sima, A., Paul, A., & Schulz, M. (2004, 23 March). The Younger Dryas - and intrinsic feature of the late Pleistocene climate change at millennial timescales. *Earth and Planetary Science Letters*, 222, 741-750.
- Stouffer, R. J., Yin, J., Gregory, J. M., Dixon, K. W., Spelman, M. J., Hurlin, W. et al. (2006, 15 April). Investigating the Causes of the Response of the Thermohaline Circulation to Past and Future Climate Changes. *Journal of Climate*, 19, 1365-1387.
- Vitart, F., Anderson, J. L., & Stern, W. F. (1997, April). Simulation of Interannual Variability of Tropical Storm Frequency in an Ensemble of GCM Integrations. *Journal of Climate*, 10, 745-760.
- Walsh, J. E., & Katzfey, J. J. (1999). The impact of climate change on the poleward movement of tropical cyclone-like vortices in a regional climate model. *Journal of Climate*, 13, 1116-1132.

- Webster, P. J., Holland, G. J., Curry, J. A., & Chang, H.-R. (2005, 16 September). Changes in Tropical Cyclone Number, Duration, and Intensity in a Warming Environment. *Science*, 309, 1844-1846.
- Wu, G., & Lau, N. (1991). A GCM simulation of the relationship between tropical-storm formation and ENSO. *Monthly Weather Review*, 120, 958-977.